Advanced Flow-Based Analysis Utilizing Spectroscopy for Biological and Environmental Samples

愛知工業大学 附属図書館 蔵書

MINORU UEDA

The Graduate School of Engineering

Aichi Institute of Technology

(Doctor course)

March 2011

Contents

Chapter 1 Introduction

Flow injection analysis (FIA) reported by Ruzicka and Hansen[1] in 1975 is one of the versatile technique for rapid and sensitive analysis. The basic flow system is shown in Fig 1-1. The system consists of a pump (P), a six-way valve (V), a reaction coil (RC) and a detector (D). The carrier and reagent solutions are pumped continuously to establish a baseline. A sample is injected into the carrier solution through V. And then the injected sample is merged with the reagent solution in RC, and the detectable reaction occurs. Finally, absorbance, fluorescence intensity and/or other response of chemical products is monitored by the detector such as spectrophotometer, fluorescence spectrophotometer and so on. FIA has advantages in the rapidity, simplicity, reduction of reagents amounts and sample volume, easy assembly and cost-performance over conventional methods.

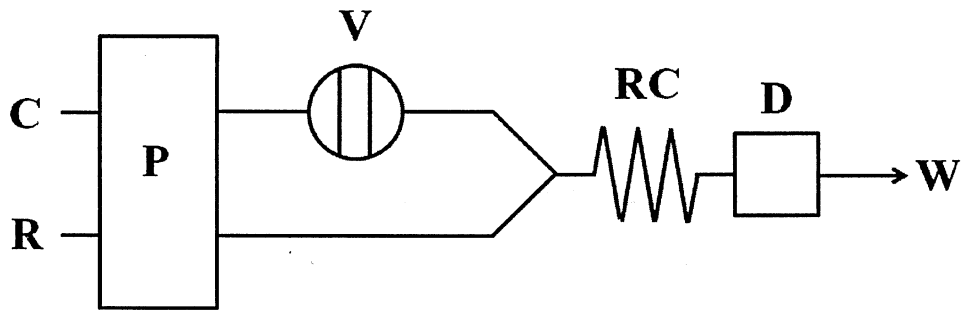

Fig. 1-1 The schematic diagram of basic flow system

P, pump; V, six-way valve; RC, reaction coil; D, detector; C, carrier; R, reagent; W, waste.

In 1990, Ruzicka *et al.* proposed sequential injection analysis (SIA)[2] as the second generation of flow analysis. Fig. 1-2 shows the diagram of SIA system. The typical SIA system is composed of a multiport selection valve (SV), a syringe pump (SP), a holding coil (HC) and a detector (D). In SIA method, microliter volumes of sample and reagents are aspirated sequentially into HC and then the product is dispensed through the detector. Therefore, the consumption of sample and reagents can be reduced dramatically compared to the conventional FIA system.

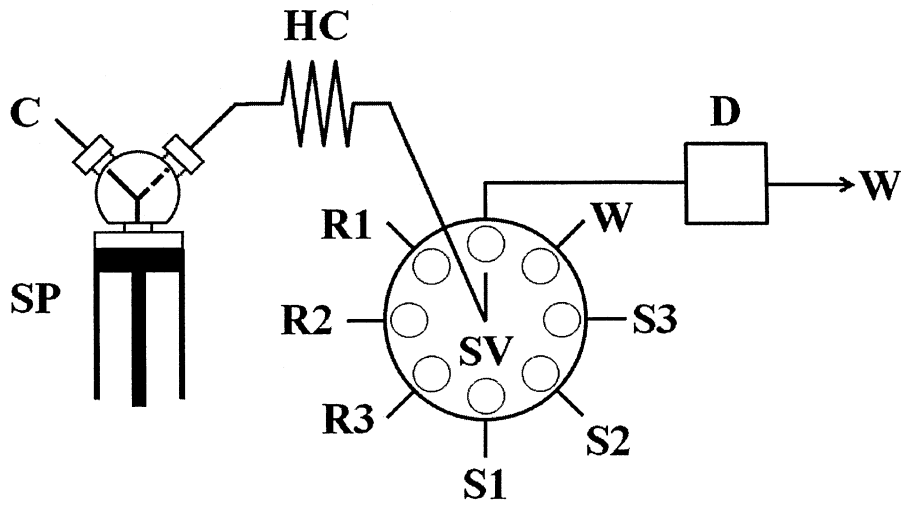

Fig. 1-2 The schematic diagram of typical SIA system.
SP, syringe pump; SV, multi-port selection valve; HC, holding coil; D, detector; C, carrier; R1,R2,R3, reagent; S1,S2,S3, standard/sample; W, waste.

In the flow-based analysis, a liquid sample is usually introduced into the system. Therefore, when a gaseous sample is analyzed by the flow-based analysis, the sample has to be absorbed into an absorber. A membrane based diffusion scrubber (DS) was proposed for sampling of the gaseous sample by Dasgupta in 1984.[3] An annular DS

consists of a porous membrane with a inner tube (MT) and a jacket tube (JT). The diagram of the annular DS is shown in Fig. 1-3. The sample gas flows between MT and JT and a gaseous sample through the membrane is collected into an absorbing solution set into MT. The volume of the absorbing solution (0.1-0.2 mL) is same as that of the sample loop of the FIA system. Therefore, the annular DS is suitable to combine with the flow based analysis and flow analyzers equipped with DS have developed for atmospheric gases.[4-7]

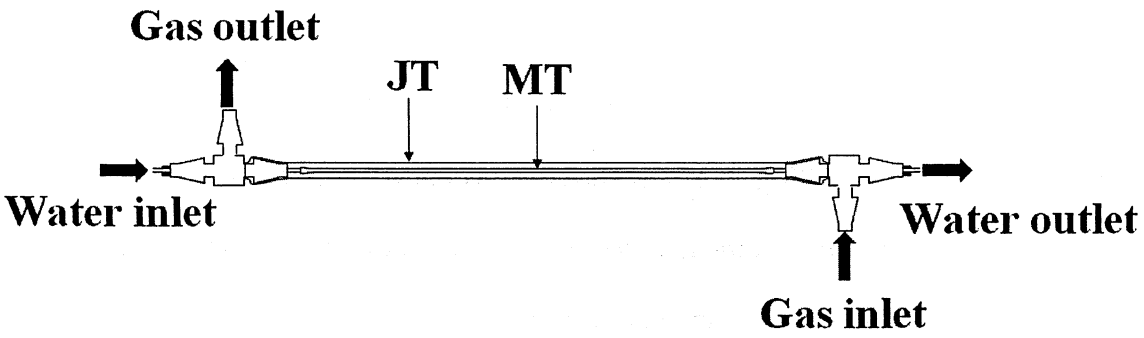

Fig. 1-3 The schematic diagram of the annular DS.
JT, jacket tube; MT, porous membrane tube

As mentioned above, FIA and SIA have numerous merits. However, these also have some disadvantages. For instance, FIA needs to propel the carrier and reagent solution continuously to obtain a stable base line. This leads a large amount of waste. Although the sample and reagent solutions in SIA are aspirated into a common HC and the reversal flow is done, the mixing efficiency is lower than that of FIA. Recently, new concepts of flow-based techniques have been proposed to enhance and to develop their function. For example, Teshima *et al.*[8] proposed an alternative concept called stopped-in-loop flow analysis (SIL-FA). In the SIL-FA method proposed, the sample

solution merges with the reagent solution and well-mixed solution is loaded into the loop. While the reaction proceeds, the solution in the loop is separated by the six-way valve from main stream and all pumps are stopped during the color development. Therefore, the net waste is zero in this period. After that, the reaction product is dispensed to the detector. This system leads a lower reagents consumption and waste generation.

To enhance the sensitivity, solid phase extraction (SPE) is widely used. However, manual SPE procedures are complicated and time-consuming because they need stepwise operations such as conditioning, sampling, eluting, and so on. Accordingly, fully automated procedure has been requested. FIA and SIA have high capabilities on automated solution handling systems such as chemical derivatization, dilution and on-line SPE. On-line pretreatment systems based on flow-based techniques coupled with spectrophotometry,[9-11] inductively coupled plasma atomic emission spectrometry (ICP-AES),[12-18] inductively coupled plasma mass spectrometry (ICP-MS),[19-23] flame atomic absorption spectrometry (FAAS)[24-30] and electrothermal atomic absorption spectrometry (ETAAS)[31-37] have been developed for sensitive and selective analysis..

However, the concept of green chemistry has become more important for the sustainable development. Especially, hazardous waste must be minimized. In general, the miniaturization of the analysis system is extremely effective in the reduction of reagents consumption and waste generation. As a result, concept of micro total analysis system (μTAS) has been proposed[38] and the analysis system called on lab-on-a-chip was investigated in many fields.[39-41] However, fabrication of μTAS usually needs high technology and expensive devices. Therefore, a simple and economic system is required.

In this dissertation, advanced flow-based analysis systems for biological and

environmental samples are proposed and their usefulness novel techniques are discussed. In the chapter 2, the FIA method for formaldehyde (HCHO) in water sample was investigated. We found that HCHO was condensed with hydroxylamineand the residual hydroxylamine after condensation reduced iron (III) complex to iron (II) complex. Therefore, HCHO can be determined with decrease in absorbance of the complex. These reactions were introduced into a three-channel FIA system and the proposed system was applied to the determination of HCHO in the wastewater sample. The proposed method is available to the monitoring of wastewater. In the chapter 3, the automated fluorimetric FIA system equipped with gas collection system using annular DS was developed. HCHO in the human breath is paied attention as a biomarker of cancer. However, simple and rapid flow system for breath HCHO has not been reported so far. In this system, the DS was used for on-line collection and concentration of breath HCHO. Furthermore, a new HCHO standard gas generator was developed and used for the calibration of the system. It is possible to check the movement on the breath HCHO concentration after smoking using the developed system. In the chapter 4, the automated stopped-in-dual-loop flow analysis (SIDL-FA) was proposed as an improved SIL-FA method. In this system, two coiled loops were set in SIL-FA system to enhance sampling rate. The developed technique gave a higher sample throughput than that of previous SIL-FA system. In addition, a programmable touchscreen controller was newly designed for an automation of the SIDL-FA operation sequence. The proposed SIDL-FA system was applied to the determination of vanadium in bottled drinking water. In the chapter 5, the automated pretreatment system equipped with a graphite furnace atomic absorption spectrometer was developed for the determination of trace cadmium and lead. Complicated manual SPE procedures were automated by the sequential injection technique. Cadmium and lead at ppt level could be determined using this

instrumentation and the sensitivity was comparable to that by ICP-MS. The proposed system was applied to the determination of cadmium and lead in leached solution from ceramic ware. Finally, an environmental-friendly acidity assay was demonstrated in the chapter 6. A miniaturized analysis system called lab-on-chip (LOC) was applied to the determination of acetic acid. The LOC is capable of cost-effective analysis and reduction of reagent consumption and waste generation. By the proposed system, waste volume was reduced dramatically than that of a traditional titration method and flow technique with titrimetry. In addition, in this detection system, an extract from flower was used as an indicator for the neutralization. We newly propose a new environment-friendly methodology with a natural and non-toxic reagent.

The developed technologies proposed here are novel and useful in the environmental and clinical fields.

Chapter 2 Flow injection spectrophotometric determination of formaldehyde based on its condensation with hydroxylamine and subsequent redox reaction with iron(III)-ferrozine complex[42]

2.1. Introduction

Formaldehyde (HCHO) is widely used as a fundamental building block for organic synthesis in industry, *e.g.* urea formaldehyde resin, melamine resin, phenol formaldehyde resin, and also it is extremely useful for disinfection in clinical field. However, exposure to HCHO in higher concentration can cause well-known effects as irritation of the eyes and upper respiratory tract, burning sensations in the mucous membrane and so on. To prevent significant sensory irritation in the general population, an air quality guideline value of 0.1 mg m^{-3} (0.08 ppmv) as a 30-minute average is recommended by the World Health Organization. [43]

On the other hand, discharge of HCHO in hydrosphere should be also paid attention. Japanese government partly revised environmental quality standards for water pollution in 2003, and HCHO was added as a monitoring substance in living environment items. [44] The guideline value is equal to or less than 1 mg L^{-1} in rivers and lakes. Industrial wastewater is discharged into water environment, so it must be strictly controlled.

Murai *et al.* [45] reported a sensitive spectrophotometry for formaldehyde in rainwater by membrane solubilization technique. In this batchwise method, HCHO was converted into a blue cationic dye with 3-methyl-2-benzothiazolinone hydrazone (MBTH), and the dye was retained on a membrane filter as an ion-associate with tetraphenylborate anion, followed by dissolving the filter in 2-methoxyethanol containing sulfuric acid to measure the absorbance at 670 nm. This method is sensitive, however such manual

procedure is time consuming and tedious.

Utilization of flow-based analysis techniques is attractive for assembling rapid, reproducible and automated analytical systems for HCHO determination. The MBTH method was introduced into FIA system for the spectrophotometric determination of HCHO in indoor and ambient air.[6] It is well-known that Hantzsch reactions are useful for the determination of HCHO.[46] A lot of spectrophotometric or fluorometric FIA methods based on the Hantzsch reactions have been reported for the determination of HCHO in atmosphere,[4] indoor air,[47] human exhaled breath,[48] natural waters[49-51] and food.[52]

Nakano *et al.*[53] developed a monitoring tape for gaseous HCHO, based on its condensation with hydroxylamine sulfate in which sulfuric acid was liberated. The porous cellulose tape was impregnated with hydroxylamine sulfate and Methyl Yellow as a pH indicator, so that the color change could be observed by the liberated sulfuric acid. However this method has not been applied to water samples.

We found that the residual hydroxylamine in the above mentioned condensation reduced iron(III) to iron(II) in the presence of 1,10-phenanthroline (phen) to produce a red iron(II)-phen complex. Since the decrease in absorbance of the complex was proportional to the concentration of HCHO, we developed a spectrophotometric FIA method for HCHO determination by monitoring the residual hydroxylamine using iron(III)-1,10-phenanthroline (phen) complex.[54]

In the present work, we investigated the other two ligands such as 2,4,6-tris(2-pyridyl)-1,3,5-triazine (TPTZ) and ferrozine in place of phen. As a result, a highly sensitive FIA method based on the condensation followed by the reduction reaction of iron(III)-ferrozine complex was developed.

2.2. Experimental

2.2.1. Reagents

All reagents were of analytical grade and used without further purification. Deionized water used to prepare solutions was obtained from an Advantec GSH-200 apparatus.

A HCHO solution (37% HCHO, 8% methanol, Nacalai Tesque, Kyoto) standardized by iodometry was used to produce a 1 w/w% (10000 mg L^{-1}) HCHO standard solution. The solution was diluted with water before use.

A hydroxylamine sulfate stock solution (1.0×10^{-2} M) was prepared by 0.16 g of hydroxylamine sulfate (Wako Pure Chemical Industries, Osaka) in 100 mL of water. Working solution of hydroxylamine was prepared by diluting the stock solution with water.

An iron(III) stock solution (2.0×10^{-3} M) was prepared by dissolving 0.0964 g of ammonium iron(III) sulfate dodecahydrate in 100 mL of 0.2 M hydrochloric acid.

1.0 M sodium acetate was mixed with 1.0 M acetic acid solution to obtain an acetate buffer solution at pH 5.

A mixed solution containing 1.6×10^{-4} M iron(III), 8.0×10^{-4} M ferrozine (Dojindo Laboratories, Kumamoto, the trade name is PDTS), and 0.1 M acetate buffer at pH 5 was daily prepared. The mixed solution constituted RS_2 referred to in the section describing the apparatus and procedure.

TPTZ purchased from Dojindo Laboratories was mixed in the reagent solution (RS_2) in place of ferrozine (eventually this ligand has not been chosen).

2.2.2. Apparatus and procedure

Fig. 2-1 shows the manifold of the FIA system assembled in this work. Flow rates of two double plunger pumps (Dual Pump 201, Intelligent Pump 301 M, FLOM, Tokyo) were set at 0.3 mL min^{-1} (0.15 mL min^{-1} for each channel, respectively). The HCHO condensation with hydroxylamine occurred in a temperature control system (S-3850, Soma Optics) which consisted of a heated reaction coil at 90°C (RC_1, 0.5 mm i.d., 8 m long) and a cooling reaction coil (CC, 0.5 mm i.d., 2 m long). A double beam spectrophotometer (S-3250, Soma Optics, Tokyo) fitted with a flow-through cell (8 μL volume, 10 mm path length) was used for the absorbance measurement. The signal was recorded on a recorder (Chino, EB 22005, Tokyo).

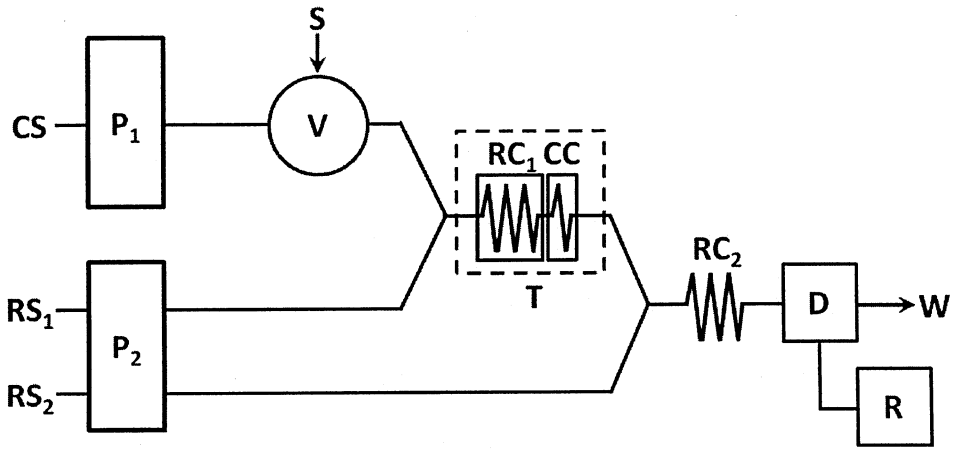

Fig. 2-1 Schematic flow diagram of the FIA system.

CS, carrier solution (H_2O); RS_1, 1×10^{-5} M hydroxylamine sulfate; RS_2, mixed solution of 1.6×10^{-4} M iron(III), 8×10^{-4} M ferrozine, and 0.1 M acetate buffer (pH 5); V, 6-way valve; S, formaldehyde standard/sample (200 μL); P_1 and P_2, double plunger pumps (0.3 mL min^{-1} each pump); T, temperature control system; RC_1, 0.5 mm i.d. ×8 m (90 °C); CC, 2 m (25 °C); RC_2, 0.5 mm i.d. ×6 m; D, spectrophotometer (562 nm); R, recorder; W, waste.

An aliquot of HCHO standard/sample (200 μL) injected into a carrier solution of water (CS) merged with 1×10^{-5} M hydroxylamine sulfate (RS_1) and with a mixed solution of 1.6×10^{-4} M iron(III), 8.0×10^{-4} M ferrozine, and 0.1 M acetate buffer at pH 5 (RS_2). The absorbance of the purple colored iron(II)-ferrozine complex was monitored at 562 nm.

2.3. Results and Discussion

2.3.1. Absorption spectra

HCHO reacts with hydroxylamine sulfate to produce formaldoxime and to liberate sulfuric acid as shown in Eq. (1):

$$2HCHO + (NH_2OH)_2 \cdot H_2SO_4 \rightleftharpoons 2H_2C{=}NOH + H_2SO_4 + 2H_2O \quad (1)$$

In this reaction, hydroxylamine decreases in proportion to the concentration of HCHO. The residual hydroxylamine reduces iron(III) to iron(II)[55]:

$$(NH_2OH)_2 \cdot H_2SO_4 + 4Fe^{3+} \rightleftharpoons N_2O + H_2O + 6H^+ + 4Fe^{2+} + SO_4^{2-} \quad (2)$$

The produced iron(II) reacts with ferrozine to form a purple iron(II)-ferrozine complex that has an absorption maximum at 562 nm:

$$Fe^{2+} + 3\text{ferrozine}^{2-} \rightleftharpoons [Fe(\text{ferrozine})_3]^{4-} \quad (3)$$

Therefore, the decrease in hydroxylamine can be monitored by measuring the decrease in absorbance at 562 nm. Preliminary batchwise study was conducted to obtain absorption spectra of the reaction products as follows. To 1.0 mL of 2.5×10^{-4} M hydroxylamine sulfate in a 10 mL volumetric flask, 0 – 2.0 mL of 5.0 mg L^{-1} HCHO standard solution was added, followed by adding 2.0 – 0 mL of water (the volume of the mixed solution was 5.0 mL each). Then, 1.0 mL of 8.0×10^{-4} M iron(III), 1.0 mL of 5.0×10^{-3} M ferrozine and 1.0 mL of 1.0 M acetate buffer (pH 5) were added. After diluting to the mark with water, the solution was allowed to stand for 20 min at room temperature. Finally the absorption spectra were measured. As shown in Fig. 2-2, the absorbance at 562 nm decreased monotonously as a function of the concentration of HCHO.

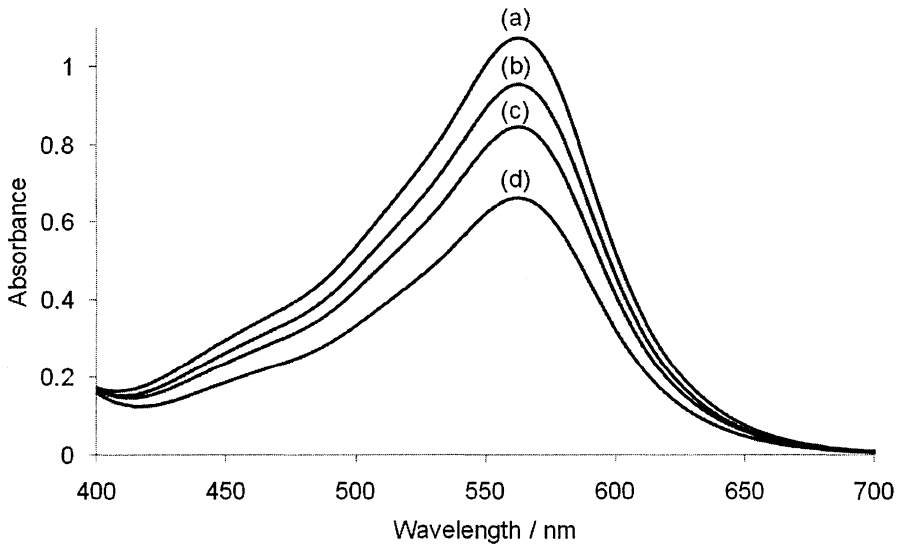

Fig. 2-2 Absorption spectra of the reaction products.

Formaldehyde concentration (mg L^{-1}): (a), 0; (b), 0.25; (c), 0.50; (d), 1.00. $C_{\text{hydroxylamine sulfate}}$, 2.0×10^{-5} M; $C_{\text{iron(III)}}$, 8.0×10^{-5} M; $C_{\text{ferrozine}}$, 5.0×10^{-4} M; $C_{\text{acetate buffer}}$ (pH 5.0), 0.1 M.

When an HCHO solution was injected into the carrier solution, the hydroxylamine concentration decreased and consequently the concentration of the produced purple complex became smaller, recording a negative peak for HCHO.

2.3.2. *Effect of ligand on the sensitivity*

In a previous paper,[54] an iron(III)-phen complex was employed in order to monitor the residual hydroxylamine which produced a red iron(II)-phen complex. The effect of ligands such as phen, TPTZ, and ferrozine were investigated on the sensitivity in this FIA system. The results together with the characteristics of their iron(II) complexes are shown in Table 2-1. When a solution of iron(III)-ferrozine complex buffered at pH 5 was delivered from RS_2, the highest negative peak for HCHO was obtained. The molar absorptivities of iron(II)-phen, -TPTZ, and -ferrozine complexes were 1.10×10^4, 2.26×10^4, and 2.79×10^4 L mol^{-1} cm^{-1}, respectively.[56] The differences in the sensitivity of this study can be attributable to the molar absorptivities. Accordingly ferrozine was chosen for the following experiments.

Table 2-1 The values of ΔAbsorbance for 0.25 mg L^{-1} formaldehyde using three ligands and characteristics of their iron(II) complexes.

Ligand	ΔAbsorbance[a]	ε[b] / L mol^{-1} cm^{-1}	λ_{max} / nm	Composition
phen[c]	$0.013\pm0.000_3$	11,100	510	$[Fe(phen)_3]^{2+}$
TPTZ[d]	$0.026\pm0.000_2$	22,600	593	$[Fe(tptz)_2]^{2+}$
Ferrozine	$0.035\pm0.000_5$	27,900	562	$[Fe(ferrozine)_3]^{4-}$

[a] Corresponded to the magunitude of the negative peaks (n = 3).
[b] Ref. 56.
[c] 1,10-Phenanthroline.
[d] 2,4,6-Tris(2-pyridyl)-1,3,5-triazine.

2.3.3. *Optimization study*

All reaction parameters were optimized using a 0.25 mg L^{-1} HCHO standard solution. The examined ranges and the chosen optimum conditions except for ferrozine concentration (its dependence is described in the next section) are summarized in Table 2-2.

Table 2-2 Examined Ranges of reaction parameters and optimum condition.

Parameter	Range	Optimum chosen
[Hydroxylamine]	2.0×10^{-6} – 8.0×10^{-5} M	1.0×10^{-5} M
[Iron(III)]	2.0×10^{-5} – 1.6×10^{-4} M	1.6×10^{-4} M
pH	3.0 – 5.0	5.0
Temperature	50 – 90°C	90°C
RC_1 length	4 – 12 m	8 m
RC_2 length	2 – 8 m	6 m
Flow rates of P_1 and P_2	0.3 – 0.9 mL min^{-1}	0.3 mL min^{-1}

2.3.3.1. *Effects of chemicals*

The magnitude of negative peak height decreased above 1×10^{-5} M hydroxylamine. Only hydroxylamine concentration of 1×10^{-5} was enough to obtain a good sensitivity. The sensitivity increased with an increase in iron(III) concentration, so an iron(III) concentration of 1.6×10^{-4} M was chosen. Ferrozine concentration was also varied, and the result is shown in Fig. 2-3. The sensitivity increased with increasing ferrozine concentration up to 4×10^{-4} M and kept nearly the same sensitivity till 1.2×10^{-3} M. Therefore, a ferrozine concentration of 8.0×10^{-4} M was chosen.

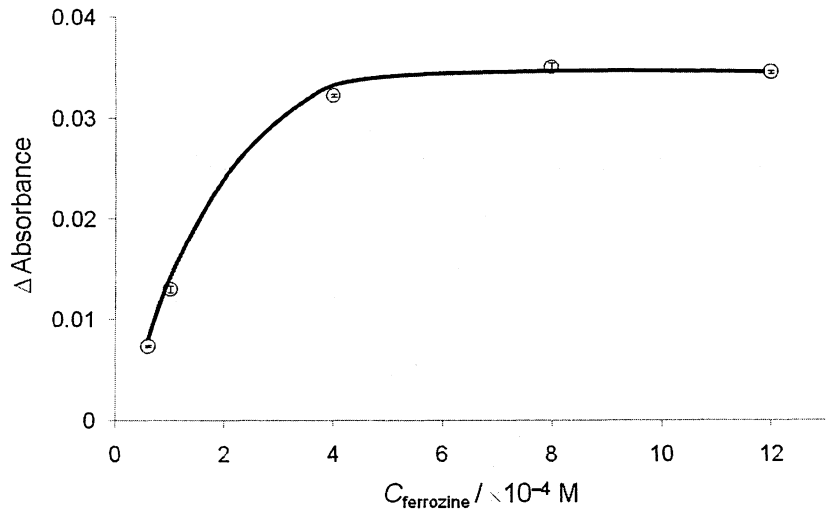

Fig. 2-3 Effect of ferrozine concentration on the determination of 0.25 mg L^{-1} formaldehyde.

2.3.3.2. Effect of pH

As expected, liberation of proton during the condensation is favorable at higher pH. Maximum sensitivity was obtained at higher pH in the examined range. A buffer solution at pH 5.0 was chosen.

2.3.3.3. Effect of temperature

Due to the very low speed of the condensation reaction occurring in the RC_1 the heater was positioned in the FIA system. Temperature setting of the temperature control system was varied in the range of 50 – 90°C. The response of HCHO monotonically increased with raising temperature. A temperature was therefore set at 90°C.

2.3.3.4. *Effects of RC_1 and RC_2 lengths*

For RC_1 in which hydroxylamine and HCHO were mixed, an 8 m-long coil (the longest coil in the examined range) was the most suitable one to help promoting the reaction. RC_2 longer than 6 m lowered the response, because the dispersion of the product occurred. An RC_2 of 6 m was therefore chosen.

2.3.3.5. *Effect of flow rate*

Flow rates of P_1 and P_2 were simultaneously varied from 0.3 – 0.9 mL min^{-1}. The highest response was obtained at a flow rate of 0.3 mL min^{-1}, and thus we chose this flow rate for each pump.

2.3.4. *Calibration curve*

The typical system output is shown in Fig. 2-4. A calibration curve was obtained in the range of 0 – 0.25 mg L^{-1} HCHO. The equation was as follows: $A = 0.174C_{HCHO} + 0.003$ with a correction coefficient of 0.994, where A is Δ absorbance and C_{HCHO} is the concentrations of HCHO in mg L^{-1}. The limits of detection (S/N = 3) and quantitation (S/N = 10) were 1.60 and 5.32 μg L^{-1}, respectively. The RSD values (n = 4 each) for the responses at 0.05 and 0.25 mg L^{-1} standards were 0.42 and 0.36%, respectively. The sampling rate is 12 samples h^{-1}.

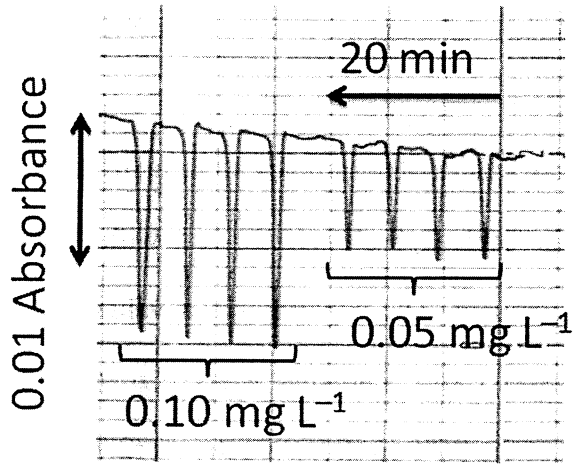

Fig. 2-4 Typical chart output for response to standard formaldehyde.

2.3.5. Interference study

The effects of some substances that often coexist with HCHO in industrial wastewater samples were studied. For the determination of 0.25 mg L^{-1} HCHO, compounds of the aldehyde and the acetone family and some metal ions were mixed. The results are shown in Table 2-3. The tested aldehydes gave serious interference. Therefore, we analyzed industrial wastewater after distillation[57] (see the next section).

Table 2-3 Tolerance limits of foreign substances or compounds on the determination of 0.25 mg L^{-1} formaldehyde.

Tolerance limit / mg L^{-1}	Added substances
50	Methyl isobutyl ketone
2	2-Butanone
0.1	Cu(II), Zn(II)
0.05	Co(II), propionaldehyde, n-butyraldehyde
0.02	Acetaldehyde

2.3.6. Application to industrial wastewater

Five distilled industrial wastewater samples were analyzed by the present method. The results are shown in Table 2-4. A paired *t*-test with 4 degrees of freedom was performed on the data obtained. The experimental *t*-value between the proposed and acetylacetone[57] methods was 1.869. Statistical analysis revealed that the critical *t*-value for 4 degrees of freedom at the 95% confidence interval (2.776) was significantly higher than the above-mentioned experimental *t*-value. This indicates that there is no significant different between the two methods.

Table 2-4 Determination of formaldehyde in industrial wastewater[a].

Sample No.	Proposed method / mg L^{-1}	Acetylacetone method / mg L^{-1}
1	157±3.7	155
2	8.58±0.07	8.24
3	12.2±0.2	11.6
4	13.4±0.1	12.1
5	12.2±0.2	12.6

[a] These samples were distilled and diluted with suitable ratio before measurement.

2.4. Conclusion

An FI method have been proposed here for the spectrophotometric determination of HCHO in industrial wastewater. It was based on the condensation of HCHO with hydroxylamine and the subsequent reduction reaction of iron(III)-ferrozine complex with the residual hydroxylamine to form a purple iron(II)-ferrozine complex (λ_{max} = 562 nm). The application data we obtained can support the utility of this method for being adopted as wastewater controls. The sensitivity of the present method (LOD = 1.6 μg

L^{-1}) is expected to be applicable to not only wastewater analysis but also natural water analysis.

Chapter 3 Formaldehyde Standard Gas Generator Based on Gravitational Dispensing-Vaporization and Its Application to Breath Formaldehyde Determination[48]

3.1. Introduction

A standard gas cylinder is usually used to calibrate an analytical instrument for gas analysis. However, a commercially available standard gas cylinder is very expensive, and the gas concentration in the cylinder is changeable with time. In addition, the standard gas must be diluted with zero gas in order to obtain an appropriate gas concentration, and the procedure for dilution is complicated. Therefore, an alternative cost-effective and easy standard gas generator has been requested. Hori *et al.*[58] developed a formaldehyde (HCHO) gas generator using solid paraformaldehyde, and Ohira *et al.*[59] developed a micro gas generator for an on-site calibration.

Generally, blood and/or urine samples are used for disease diagnosis and a physical checkup in clinical laboratories. Recently, however, breath analysis has been paid attention as a noninvasive diagnosis.[60,61] Metabolites produced in the human body are circulated by bloodstream, and volatile organic compounds (VOCs) among the metabolites are excreted to the breath through the alveoli. Major VOCs in breath are isoprene (12-580 ppbv), acetone (1.2-880 ppbv), ethanol (13-1000 ppbv) and methanol (160-2000 ppbv).[62] Some of them are related to specific diseases. For example, the acetone concentration in the breath from the diabetic patient is higher than that from the healthy person.[63]

Gas chromatography-mass spectrometry (GC-MS) is widely used for breath analysis.[64,65] Phillips *et al.*[66] analyzed the breath from an individual subject (n = 50)

using GC-MS and detected the average about 200 VOCs. Fourier transform-infrared (FT-IR),[67,68] proton transfer reaction-mass spectrometry (PTR-MS)[69,70] and selected ion flow tube-mass spectrometry (SIFT-MS) [71-73] have been also used for breath analysis. These instrumental analyses are suitable for multi VOCs analysis, however, for single VOC analysis, a simpler analytical system is desired.

There have already been some reports on the determinations of principal breath VOCs: acetone with salicylaldehyde,[74] ammonia with a liquid-film conductivity sensor,[75] and isoprene using a gas phase reaction with ozone.[76] Also, breath hydrogen peroxide was determined using chemiluminescence.[77] However, a convenient flow injection method for the determination of breath HCHO has not yet been reported.

It was reported that the HCHO concentrations in headspace of urine from the patients suffering from bladder or prostate cancer were higher than those from healthy persons.[78] Moreover, Wehinger *et al.*[79] suggested that HCHO in exhaled breath may be useful for diagnosis of lung cancer. Therefore, the breath HCHO is expected as a biomarker of the cancer.

Sakai *et al.*[47] developed a fluorimetric flow injection method for the determination of gaseous HCHO in indoor environment using 5,5-dimethylcyclohexane-1,3-dione (dimedone). However, an off-line sampling procedure using impingers was exploited before flow injection measurement.

In this study, a new HCHO standard gas generation method is developed, and a rapid and simple fluorimetric flow injection analysis (FIA) system coupled with a porous membrane based diffusion scrubber (DS) is proposed for the determination of breath HCHO.

3.2. Experimental

3.2.1. *Apparatus*

A diagram of the FIA system in this study is shown in Fig. 3-1.

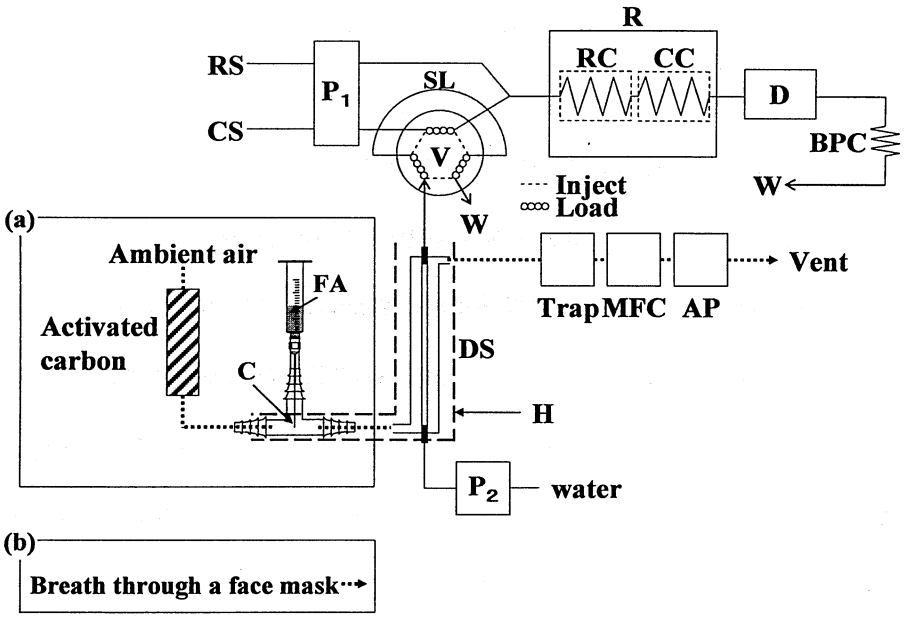

Fig. 3-1 Automated FIA system for gaseous formaldehyde.

CS, Carrier solution (distilled water); RS, Reagent solution (0.3 % dimedone in acetate buffer); P_1, Double plunger pump (1.4 mL / min); V, Six way valve; SL, Sample loop (300 μL); R, Reaction system; RC, Reaction coil (i.d. 0.5 mm × 7 m, 135 °C); CC, Cooling coil (i.d. 0.5 mm × 2 m); D, Fluorescence spectrophotometer (EX: 395 nm, EM: 463 nm); BPC, Back pressure coil (i.d. 0.25 mm × 2 m); W, Waste; FA, Formaldehyde solution; C, Capillary tube (i.d. 0.03 mm); MFC, Mass flow controller (0.4 SLPM); H, Heater (Broken line, 40 °C); P_2, Peristaltic pump; DS, Diffusion scrubber; AP, Air pump; (a), instrument calibration; (b), breath analysis.

A double plunger pump (P_1) (PD-2000, FIA Instruments Co., Ltd.) was used to deliver carrier and reagent solutions. An automatic pretreatment system (Ogawa & Co., Ltd.) is equipped with a peristaltic pump (P_2) and a six-way injection valve (V). A reaction

system (R) (S-3850, Soma Optics)[47] was used to promote the derivatization reaction. The fluorescence intensity was measured by a fluorescence detector (D) (FP-2020 plus, JASCO), and the detector output was acquired on a PC through a chromatomonitor (Nippon Filcon Co., Ltd.). All liquid flow lines were made from 0.5 mm i.d. PTFE tubing except that a backpressure coil consisted of 0.25 mm i.d. PTFE tubing, and 4 mm i.d. silicone tubing was used for the gas sampling line. A gas sample was introduced to the DS by an air sampler (AP) (S-21, KOMYO RIKAGAKU KOGYO K.K.). The flow rate of gas sample was controlled using a mass flow controller (MFC) (8100MC-1, KOFLOC). The entire gas sampling line including DS was heated at 40 °C by a flexible heating tape (H) (FHU-8, TAIKA DENKI Co., Ltd.). The DS was composed of PTFE tubing (3 mm i.d.) and porous PTFE tubing (POREFLON TB-0201, Sumitomo Electric Fine Polymer, 1 mm i.d., 30 cm long).[7] The sample gas was flowed between the gap of the both tubings, and water was loaded into the porous PTFE tubing to collect the sample gas.

3.2.2. Reagents

All reagents were prepared with deionized water purified by an Advantec Aquarius GSH-200 system.

A 1 % HCHO standard solution was prepared from a HCHO solution (Nakarai tesque, Kyoto) standardized by iodometry. Working standard solutions were daily prepared with water.

A 12.5 % acetic acid solution was prepared by diluting 12.5 mL of acetic acid (Nakarai tesque, Kyoto) to 100 mL with water.

A 12.5 % ammonium acetate solution was prepared by dissolving 12.5 g of

ammonium acetate (Sigma Aldrich Japan, Tokyo) with 100 mL of water.

An acetate buffer solution (pH 5.0) was prepared by mixing 12.5 % acetic acid solution and 12.5 % ammonium acetate solution.

A 0.3 % dimedone solution was prepared by dissolving 0.6 g of dimedone (Tokyo Kasei, Tokyo) with 200 mL of acetate buffer.

3.2.3. Procedure

In the flow system as shown in Fig. 3-1, carrier and reagent solutions were continuously propelled, and also standard/sample/zero gas was continuously introduced into the DS. An automated analytical procedure was carried out by switching V and P_2 (on/off). Table 3-1 shows a protocol for the automated procedure.

Table 3-1 FIA protocol for measurement of gaseous formaldehyde.

	Mode			
	Filling up DS with water	Collection of sample gas	Loading of sample into loop	Injection of sample to flow system and washing DS
V	Inject	Inject	Load	Inject
P_2	on	off	on	on
Working time	30 s	1 min	30 s	1 min

Abbreviations (DS, V and P_2) as in Fig. 3-1.

First, V is positioned at "Inject" mode, and P_2 is turned on, so that water is loaded into DS by P_2. And then, P_2 is turned off, and the flow of water in the DS is therefore stopped. In this period, gasous HCHO in a sample is collected into water through the tubular porous PTFE membrane. After the sampling for 1 min, V is turned to "Load" mode, and P_2 is turned on for loading the water containing HCHO into the sample loop

on V. After that, V is turned to "Inject" mode, and the collected sample is injected into the stream of carrier solution. The fluorescence intensity of the fluorescent derivative is measured at the excitation wavelength of 395 nm and the emission wavelength of 463 nm.

3.3. Results and Discussion

3.3.1. HCHO standard gas generation method

HCHO standard gas was generated by complete vaporization of an HCHO standard solution dispensed gravitationally via a fused silica capillary tip. This method was referred to as gravitational dispensing-vaporization method. A schematic diagram of the standard gas generator is shown in Fig. 3-2.

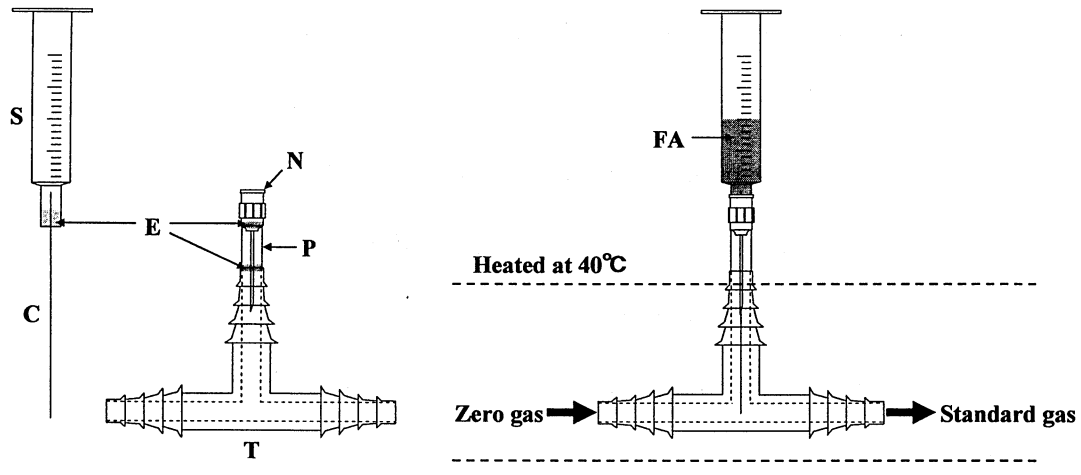

Fig. 3-2 Schematic representation of the standard gas generation part.

S: Syringe, C: Capillary tube (i.d. 0.03 mm), N: Needle, P: Polypropylene tube, T: Tee, E: Epoxy adhesive, FA: Formaldehyde solution ranged from 0.005 to 0.2 w/v%.

A fused silica capillary tube (7.5 cm long, i.d. 0.03 mm) was fixed on a 2-mL Terumo® syringe by epoxy adhesive. A HCHO standard solution filtered by a membrane filter (0.45 μm) was transferred into the syringe. The capillary was passed through a needle and affixed to the needle housing body, so that the end of capillary can be placed at the needle tip from which the HCHO standard solution can be volatilized at 40°C. The syringe was kept vertically to dispense the HCHO standard solution by gravity. Ambient air purified through a column packed with activated carbon (zero gas) was aspirated from one side of a tee-arm, and then the zero gas merged with vaporized HCHO. The concentration of the standard gas generated by this method was calculated from the following equation:

$$C_1 = \frac{F_1 \times C_2}{30.03} \times \frac{1}{F_2} \times 22.4 \qquad (1)$$

where C_1 is the concentration of the HCHO standard gas in ppbv, C_2 is the concentration of the HCHO standard solution dispensed via the fused silica capillary in g/L, F_1 is the flow rate of the HCHO standard solution dispensed via the fused silica capillary in μL/min, and F_2 is the flow rate of the HCHO standard gas in standard liters per minute (SLPM). The concentration of the HCHO standard gas in ppbv can be defined by the concentration of the HCHO standard solution in the Terumo syringe, provided F_1 and F_2 are constant.

The value of F_1 was measured by the following way. The same aliquots of water were transferred into two Terumo syringes (1 and 2) equipped with capillary tubes. The two syringes were weighed; the weight values of the syringes 1 and 2 are w_1 and w_2, respectively, in equation (2). The two syringes were kept vertical for approximately 5

hours. The water in the syringe 1 was dispensed by gravity, and also the water was slightly vaporized (lost) from the upper side of syringe. On the other hand, since one edge of the capillary tube of the syringe 2 was plugged with adhesive, the water in the syringe 2 was therefore not dispensed by gravity, but the water was slightly lost by vaporization. After approximately 5 hours, the two syringes were weighed again, and the values of weight, w'_1 and w'_2, were obtained. Assuming that the water and the HCHO standard solution are dispensed gravitationally at the same flow rate, the flow rate of HCHO standard solution through the capillary tube can be estimated from equation (2):

$$F_1 = \frac{(w_1 - w'_1) - (w_2 - w'_2)}{t} \qquad (2)$$

where t is the time for standing the syringe vertically. The numerator in equation (2) is the dispensed net water mass which is corrected by subtracting the loss of water mass vaporized from the syringe. As a result, the flow rate of HCHO standard solution through the capillary tube was 39.5 nL/min (the density of water : 1.00 g/cm^3). F_2 was maintained at 0.4 SLPM by MFC. Therefore, 73.7 ppbv of HCHO standard gas can be generated using 1.00 g L^{-1} of HCHO standard solution.

3.3.2. *Verification of the proposed standard HCHO gas generator by 2,4-dinitrophenylhydrazine (DNPH) -HPLC*

The standard gas generated by the proposed method was collected into a DNPH cartridge (LpDNPH S10L, SPELCO). And then, the collected HCHO was eluted by

acetonitrile. The eluent was analyzed by an HPLC equipment. The results are shown in Table 3-2. The concentrations of two different solutions calculated from equation (1) were 73.7 and 147 ppbv, respectively. Both theoretical concentrations were in good agreement with the analytical values by DNPH-HPLC method.

Table 3-2 Verification of the proposed standard HCHO gas generator by DNPH-HPLC.

Standard	Concentration of gaseous formaldehyde[a] / ppbv	
	Computed value	DNPH-HPLC
1[b]	73.7	75.9
2[c]	147	146

DNPH-HPLC, 2,4-dinitrophenylhydrazine-HPLC method.
a) Generated by this method based on gravitational dispensing-vaporization.
b) 0.100% formaldehyde solution was gravitationally introduced.
c) 0.200% formaldehyde solution was gravitationally introduced.

3.3.3. Optimization of the FIA system

The optimization of the FIA system was carried out using 50 μg/L of HCHO standard solution (not the standard gas).

The reaction of HCHO with dimedone occurs in the presence of ammonium acetate. Therefore, the buffer solution was prepared by mixing acetic acid and ammonium acetate solutions, and the concentration of the buffer solution was varied from 5 to 15 %. The fluorescence intensity increased with increasing the buffer concentration, but the baseline drifted at higher concentration. In this study, 12.5 % acetate buffer was selected.

The effect of pH of the buffer was examined in the range of 4.0 to 6.0. The pH of the buffer was adjusted by mixing acetic acid and ammonium acetate solutions. The

maximum fluorescence intensity was obtained at pH 5.0.

The concentration of dimedone was varied from 0.1 to 0.5 %. A 0.3 % of dimedone solution gave the maximum sensitivity.

The effect of reaction temperature was investigated. The temperature of the reaction coil in the reaction system was varied in the range of 120 to 140 °C. The fluorescence intensity increased with raising the reaction temperature, however, the baseline became noisy at higher temperature values. Considering stability of the baseline and sensitivity, the optimum reaction temperature was set at 135 °C.

The reaction coil length was varied from 5 to 9 m. A 9 m long reaction coil gave the highest sensitivity, but the baseline became unstable. Consequently, a 7 m long reaction coil was chosen. The flow rate of the carrier and the reagent solution was varied from 0.6 to 1.1 mL/min. An optimum flow rate of 0.7 mL/min was selected.

3.3.4. Calibration curve

Under the optimum conditions, the calibration curve for gaseous HCHO was prepared. The curve was linear in the range of 3.68 to 147 ppbv. The equation was $Y = 4.03X + 0.490$ with a correlation coefficient of 0.999, where Y is the relative fluorescence intensity and X is the concentration of the gaseous HCHO in ppbv. Fig 3-3 shows the observed system outputs for various standard gases. The RSD values ($n = 4$ ea.) for the responses at 3.68, 7.37, 73.7, and 147 ppbv were 5.8, 1.7, 0.9, and 0.9 %, respectively. The limit of detection (3σ) was 0.16 ppbv and the limit of quantitation (10σ) was 0.54 ppbv. The analysis time from the collection of the gaseous sample to the detection of the peak was approximately 3 min. Thus, the system is applicable for the rapid gaseous HCHO analysis.

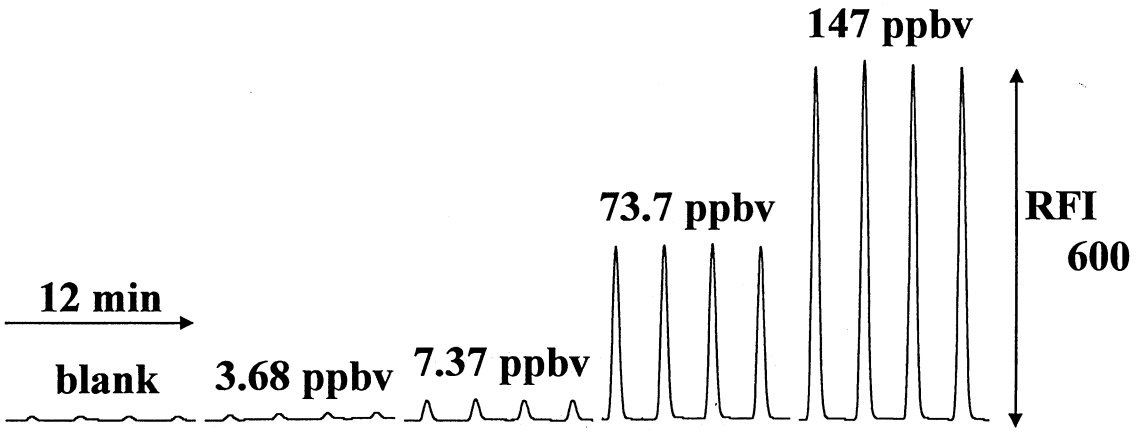

Fig. 3-3 Typical system outputs for gaseous formaldehyde generated by gravitational dispensing-vaporization format.

3.3.5. Interference study

The interferences of contaminated compounds on the determination of 50 μg/L HCHO in aqueous solution were studied. An error of less than ±5 % was considered to be tolerable on each fluorescence intensity measurement. In this study, DS was not used. The HCHO standard solution contained various contaminated compounds was injected into the carrier stream by V. The results are shown in Table 3-3. Acetaldehyde (CH_3CHO) showed the most serious interference on the determination of HCHO. It is reported that concentrations of HCHO and CH_3CHO in the breath are about 10 ppbv and 20 ppbv, respectively.[80] And Diskin *et al.*[81] reported the CH_3CHO concentration in the exhaled breath was 2-5 ppbv. From these reports, if the breath contains same level HCHO and CH_3CHO, and collection efficiencies of these aldehydes are the same, the contaminated CH_3CHO might give an error of about 10 % in this system. However, a previous work[6] using the same porous PTFE membrane tube showed that the

permeability of gaseous CH_3CHO was one hundredth compared with that of the gaseous HCHO. Therefore, it is considered that the breath CH_3CHO at the same level does not serious interfere on the determination of the breath HCHO.

Table 3-3 Effect of contaminated compounds on the determination of 50 μg/L of formaldehyde in aqueous solution.

Tolerance limit / mg/L	Added compound
10000	Methanol, Ammonia
1000	Ethanol, Acetone
250	MIBK
200	Isoprene
50	2-Butanone
0.1	Butyraldehyde
0.05	Propionaldehyde
0.02	Acetaldehyde

MIBK, methyl isobutyl ketone.

3.3.6. Detemination of the breath HCHO

Breath samples from four volunteer subjects were analyzed. A gas mask (No.6000DDSR, Sumitomo 3M) was used for sampling. The mask was connected to DS using silicone tube, and the breath sample was aspirated through DS (Fig. 3-1(b)). The four volunteers were nonsmoker and they did not suffer from any disease. The results are shown in Table 3-4. The concentrations of breath HCHO from the volunteers were in the range of 5.8 – 11.8 ppbv.

Next, the effect of smoking on the concentration of breath HCHO was investigated. Fig. 3-4 shows the system outputs for exhaled breath before and after smoking. The average breath HCHO concentration before smoking was 7.3 ppbv. After smoking, the breath HCHO concentration ranged from 10.6 to 12.5 ppbv for 25 min, and then the

concentration returned to the initial level 30 min later.

The proposed analytical system is able to analyze breath HCHO variation with smoking.

Table 3-4 Determination of breath formaldehyde.

Volunteer	Formaldehyde / ppbv[a)]	
	Jul. 31st b)	Aug. 2nd b)
A	10.4±0.4	7.3±0.2
B	8.0±0.1	7.6±0.3
C	10.9±0.7	5.9±0.3
D	11.8±0.5	5.8±0.1

a) Four determinations.
b) Sampling date.

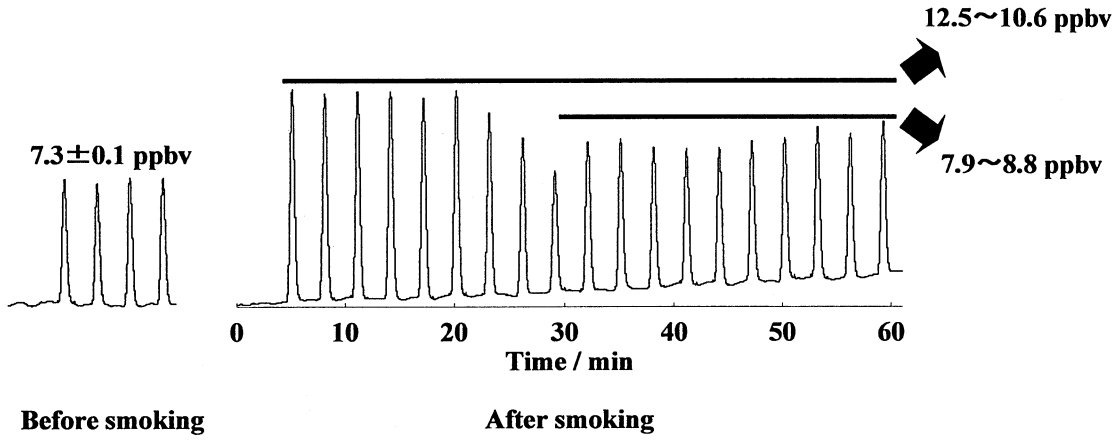

Fig. 3-4 System outputs for exhaled breath before and after smoking.

3.4. Conclusion

In this study, a reliable HCHO standard gas generation method was developed based

on the gravitational dispensing-vaporization of which reliability was confirmed by the DNPH-HPLC method. And the automatic DS collection-fluorimetric FIA system for gaseous HCHO was proposed. The trace gaseous HCHO can be measured by 3 min intervals using this system. The proposed system can be applied to the determination of the breath HCHO before and after smoking. Hereafter, it is expected that this system could elucidate the relation between drinking and eating and the breath HCHO. And the gravitational dispensing-vaporization method is also expected to be applied to the standard gas generation method for other volatile compounds.

Chapter 4 Automated stopped-in-dual-loop flow analysis system for catalyt determination of vanadium in drinking water[82]

4.1. Introduction

Vanadium has recently attracted much attention for its potential role again diabetes.[83,84] Heyliger *et al.* reported that vanadate (vanadium in pentavalent stat appeared to have an insulin-like action in the *in vivo* experiments on diabetic rats. Vanadyl (vanadium in tetravalent state) *in vitro* and in animal models of diabetes h been shown to reduce hyperglycemia and insulin resistance.[86] Some clinical trials wi human have also shown that vanadium improved insulin sensitivity in patients wi diabetes mellitus.[87] A recent study revealed that vanadium administration in impair glucose tolerance patients increased triglyceride concentrations without changes insulin sensitivity.[88]

Nowadays prevalence of diabetes is a global issue,[89] and the Japanese governme enacted the Health Promotion Act (Act No. 103 of 2002) to raise health awareness l Japanese people. We have now various kinds of bottled mineral waters as drinki waters. Some of them contain naturally occurring vanadium, and it was reported that t consecutive administration of such drinking water (containing approximately 65 μg I vanadium) might result in a significant reduction of blood glucose levels in hum diabetes.[90] Although devotees may benefit from such mineral waters with respect their health, the exact role of vanadium has yet to be established. Therefore, t concentration of vanadium in bottled mineral waters must be strictly controlled, and affordable and sensitive analytical method for vanadium determination is required.

Kinetic methods based on catalytic reactions are among the most sensitive for tra

metal analysis.[91,92] Various catalytic reactions have heretofore been utilized as indicator reactions for the determination of trace vanadium.[93-97]

FIA is one of the promising techniques to obtain highly sensitive methods, provided that suitable chemical reactions are introduced into FIA.[98] Since Yamane and Fukasawa first adapted a catalytic effect of vanadium into an FIA system,[99] several workers have described FIA methods for catalytic determination of vanadium with spectrophotometric[100-106] and chemiluminescent[107,108] detections. However, basically FIA techniques need to establish a baseline continuously, which leads to continuous waste generation.

Since Ruzicka and Hansen conceived FIA,[1] some highly sophisticated flow-based analytical systems have been proposed: air-carrier continuous analysis system,[109] sequential injection analysis,[2] multi-commutation in flow analysis,[110] multi-syringe flow injection analysis,[111] all injection analysis,[112] multi-pumping in flow analysis[113] and hybrid flow analyzer.[114] These techniques are capable of lower reagent(s) consumption and lower waste generation than traditional FIA. A multi-pumping flow system was demonstrated in relation to a spectrophotometric catalytic determination of iron and vanadium.[115]

Stopped flow injection (FI) technique allows longer reaction time with minimization of dilution and without a long reaction coil, yielding higher sensitivity as well as lower waste generation. However, conventional stopped FI systems are subject to continuous contact of the resulting solution to the cell window. This may cause violation of cleanliness on the window; especially it would be a serious problem in spectrophotometric flow-based analysis. Another concept for stopped FI procedure was proposed by Grudpan[116]: the flow is stopped at a mixing coil (not at a flow cell) for a period before allowing to flow further to the flow-through cell in a simple colorimeter

as a detector. Indeed the procedure doesn't expose continuously the cell window to the colored product, but the reagent solution continues to exist inside the cell during the stopping time.

In a previous paper,[8] an alternative stopped flow technique called stopped-in-loop flow analysis (SIL-FA) was proposed and an SIL-FA method for the catalytic determination of vanadium was demonstrated. The SIL-FA system allowed its own detection window to be washed (no continuous exposure to the reaction product and the reagents) when the reactant stayed at the stationary coiled loop on a six-way injection valve. However, the SIL-FA protocol containing switching of two six-way valves and control of three pumps (ON/OFF) were all carried out manually. Also, a produced dye in the loop was dispensed to the detector by the mixed solution containing carrier and all reagents solutions. Furthermore the applicability was limited due to only one loop in which the reaction took place.

In the present paper, two coiled loops are set in a SIL-FA system, and it was referred to stopped-in-dual-loop FA (SIDL-FA). A programmable touchscreen controller for a SIDL-FA system is newly designed, and the controller successfully accomplishes a SIDL-FA protocol for the catalytic determination of vanadium. A diluted nitric acid solution (not all reagents) is used to dispense a reaction product to the detector, so that it can minimize the consumption of reagents.

4.2. Experimental

4.2.1. Reagents

All reagents were of analytical grade and were used without further purification.

Deionized water used to prepare solutions was obtained from an Advantec GSH-210 apparatus.

A commercially available vanadium(V) standard solution for atomic absorption spectrometry (Wako, Osaka) containing 1000 mg L^{-1} vanadium (ammonium metavanadate in 0.45 M sulfuric acid) was used as a stock solution. Each working solution was prepared by serial dilution of the standard solution with 10 mM nitric acid.

A 0.25 M *p*-anisidine stock solution was prepared by dissolving 6.16 g of *p*-anisidine (99%, FW = 123.16, Alfa Aesar Johnson Matthey Japan, Tokyo) in 200 mL of 3 M hydrochloric acid. A 2 M acetate buffer solution (pH 3.3) was prepared from solutions of acetic acid (Nacalai Tesque, Kyoto) and sodium acetate trihydrate (Nacalai Tesque). These stock solutions were daily mixed to prepare a solution containing 80 mM *p*-anisidine and 1 M acetate buffer, and the mixed solution was adjusted to pH 3.3 with 10 M sodium hydroxide (Nacalai Tesque). The mixed solution constituted RS_1 referred to in the section describing the procedure.

A 50 mM bromate solution was daily prepared by dissolving 0.418 g of potassium bromate (FW = 167, Wako) in 50 mL of water.

A 0.15 M Tiron solution was daily prepared by dissolving 2.49 g of 1,2-dihydroxy-3,5-benzenedisulfonic acid disodium salt monohydrate (FW = 332, Dojindo Laboratories, Kumamoto, Japan) in 50 mL of water.

4.2.2. Apparatus

The SIDL-FA system is shown schematically in Fig. 4-1. Three double plunger micro pumps were used to deliver solutions: P_1 and P_3 were of F·I·A Instruments, Tokyo (Dual Pump 201), and P_2 was of Soma Optics, Tokyo (Intelligent Pump 301 M). A

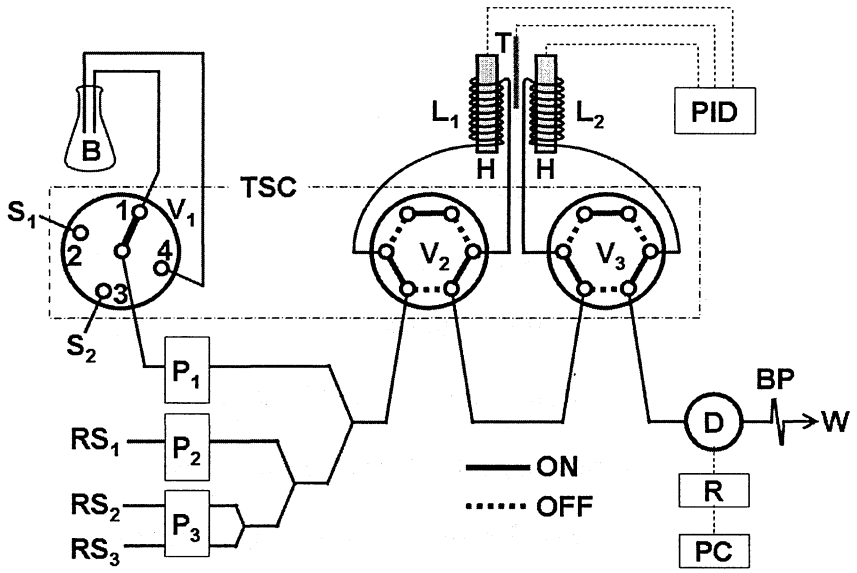

Fig. 4-1 Schematic flow diagram of the SIDL-FA system.

B, 10 mM HNO_3; S_1, and S_2, sample; RS_1, mixed solution of 80 mM *p*-ansidine and 1 M acetate buffer (pH 3.3); RS_2, 50 mM $KBrO_3$; RS_3, 0.15 M Tiron; V_1, four-port selection valve; V_2 and V_3, six-way injection valves; P_1, P_2 and P_3, double plunger pumps (P_1, 0.90 mL min^{-1} ; P_2, 0.15 mL min^{-1} ; P_3, 0.20 mL min^{-1}); H, heater; T, thermocouple; PID, proportional–integral–derivative controller (set at 105°C); L_1, first loop (100 μL); L_2, second loop (100 μL); D, spectrophotometer (510 nm); R, recorder; PC, personal computer; BP, back pressure restrictor (0.25 mm i.d., 45 cm long).

homemade touchscreen controller (TSC) possessed a four-port selection valve and two six-way injection valves. A proportional–integral–derivative (PID) digital controller (SR91, Shimaden, Tokyo) was employed to control two cartridge heaters (C3JX4A, Watlow Japan, Tokyo) with a thermocouple (type K chromel–alumel, Sakaguchi E.H VOC, Tokyo). Each heater was installed into a tubular brass that Teflon tubing was coiled to compose a heated loop. A double beam spectrophotometer (S-3250, Soma

Optics) fitted with a flow-through cell (8 μL volume, 10 mm path length) was used for absorbance measurement. The detector output was acquired on a PC through a recorder (FIA monitor, Ogawa & Co., Kobe, Japan). All flow lines were made from 0.5 mm i.d. Teflon tubing except for a backpressure restrictor (BP) that consisted of 0.25 mm i.d. Teflon tubing (45 cm long).

4.2.3. Procedure

A 10 mM nitric acid solution (B) for uncatalyzed reaction (blank measurement) or a standard/sample solution (S_1 or S_2) for catalyzed reaction was delivered by pump 1 (P_1) at a flow rate of 0.90 mL min^{-1}. This diluted nitric acid (B) was also used as a carrier solution (for dispensing a reaction product to the detector, *vide infra*). Pump 2 (P_2, 0.15 mL min^{-1}) was used to deliver a mixed solution (RS_1) of 80 mM *p*-ansidine and 1 M acetate buffer (pH 3.3). The oxidant (RS_2, 0.05 M $KBrO_3$) and the activator (RS_3, 0.15 M Tiron) solutions were delivered by pump 3 (P_3) at a flow rate of 0.1 mL/min, respectively.

As shown in Fig. 4-2, TSC controlled three pumps (P_1, P_2 and P_3), three valves (V_1, V_2 and V_3) and a recorder (R) using a built-in programmable logic controller (PLC). The temporal operation and each function of the SIDL-FA system are depicted in Table 4-1. This protocol was automatically carried out to obtain two peaks derived from two loops (L_1 and L_2). When a couple of peaks for uncatalyzed reaction (namely blank peaks) was obtained, the port No. of V_1 was fixed at 1 through one protocol (see Table 1). For a couple of peaks for catalyzed reaction, several ports of V_1 were selected.

Here a typical sequence of operation for catalyzed reaction is described. Steps 1 and 2 involve the loading of a well mixed solution of standard/sample and reagents into L_1

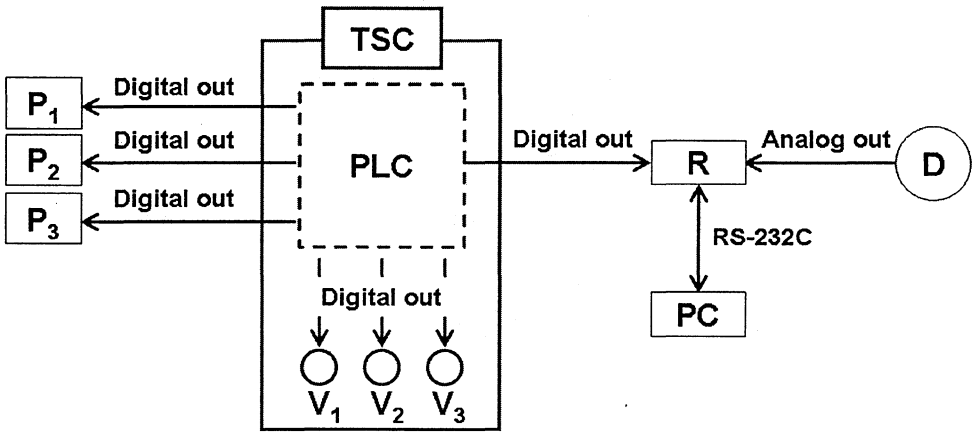

Fig. 4-2 Schematic diagram of control system with touchscreen controller (TSC). PLC, programmable logic controller. Other abbreviations as in Fig. 1.

Table 1 Temporal operation of the SIDL-FA system.

Step	Port No. of V_1		V_2	V_3	P_1	P_2	P_3	R	Time/sec	Function
	Uncatalyzed	Catalyzed								
1	1	2	ON	OFF	ON	ON	ON	OFF	75	Loading reagents and B or S_1 into L_1
2	1	3	OFF	ON	ON	ON	ON	OFF	75	Reaction in L_1, and loading reagents and B or S_2 into L_2
3	1	4	OFF	OFF	ON	OFF	OFF	OFF	40	Reaction in both loops and washing line
4	1	4	OFF	OFF	OFF	OFF	OFF	OFF	25	Reaction in both loops (net waste = 0)
5	1	4	OFF	OFF	ON	OFF	OFF	OFF	20	Reaction in both loops and establishing baseline
6	1	4	OFF	OFF	ON	OFF	OFF	ON	20	Reaction in both loops and starting data acquisition
7	1	4	ON	OFF	ON	OFF	OFF	ON	75	Reaction in L_2, signal monitoring for L_1 peak
8	1	4	ON	ON	ON	OFF	OFF	ON	40	Signal monitoring for L_2 peak

Abbreviations (V_1, V_2, V_3, P_1, P_2, P_3, R, B, S_1, S_2, L_1,and L_2) as in Fig. 1.

and L_2. The catalyzed reaction at 105°C occurs in L_1 (steps from 2 to 6) and L_2 (steps from 3 to 7) for 180 sec, respectively. While the reaction occurs in each loop, the flow-through cell and the flow line are washed with a diluted nitric acid (B) to prevent

continuous exposure to the reaction product and the reagents (step 3). The net waste is zero in step 4 (all pumps are turned off). In step 5, a baseline is established by pumping only B (only P_1 is turned on). In step 6, a trigger is sent to the recorder to acquire data. Finally, a peak for L_1 is obtained in step 7, followed by step 8 for signal monitoring of a peak for L_2. The overall measurement cycle for the two peaks requires therefore 370 s.

The absorbance of the reaction product was measured at 510 nm.

4.3. Results and Discussion

4.3.1. Absorption spectra

The chemistry relied on the catalytic effect of vanadium on the oxidation reaction of *p*-anisidine by bromate in the presence of Tiron as an activator. Preliminary batchwise experiments have been conducted to obtain absorption spectra. The procedure was as follows: to 5 mL of 50 mM *p*-anisidine in a 25-mL of volumetric flask, 0.5 mL of 2 M acetate buffer, 4 mL of 2.5 μg L^{-1} vanadium(V) in 10 mM nitric acid (or same volume of 10 mM nitric acid for blank) and 1 mL of 0.25 M Tiron were added. Then after adjusting pH 3.3, the solution was kept at 65°C in a thermostated bath for about 5 min to attain thermal equilibrium. To initiate the catalytic reaction, 1 mL of 0.25 M bromate heated at 65°C was added, and diluted to the mark with water. At 30 min after the initiation of the reaction, a portion of the sample solution was transferred into a test tube, and the test tube was immersed in an ice bath about 30 s for quenching. The observed absorption spectrum is shown in Fig. 4-3. The red colored product has an absorption maximum at 510 nm.

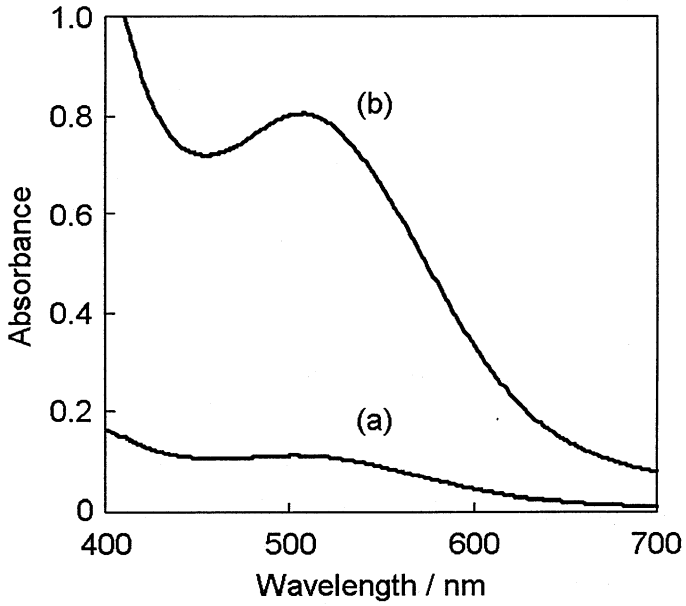

Fig. 4-3 Absorption spectra of the reaction product.

C_V in μg L^{-1}: (a), 0; (b), 0.4. $C_{p\text{-anisidine}}$, 10 mM; $C_{\text{acetate buffer}}$, 40 mM (pH 3.3); C_{Tiron}, 10 mM; C_{bromate},10 mM; temperature, 65°C; reaction time, 30 min.

Bontschev and Jeliazkowa[117] fully investigated the catalytic oxidation of *p*-phenetidine (NH_2-Ph-OC_2H_5) by chlorate with vanadium(V) as catalyst. They reported that vanadium(V) forms a charge transfer complex with NH_2-Ph-OC_2H_5, an electron from the arylamine is completely localized in an atomic orbital of vanadium, and two arylamine radicals are formed:

$$V(V) + NH_2\text{-Ph-}OC_2H_5 \rightleftharpoons [V(V) \leftarrow\cdots NH_2\text{-Ph-}OC_2H_5] \longrightarrow$$
$$V(IV) + H^+ + \dot{N}H\text{-Ph-}OC_2H_5 \longleftrightarrow NH\text{-}\dot{P}h\text{-}OC_2H_5 \quad (1)$$

Finally *N*-(4-ethoxyphenyl)-quinoneimine (λ_{max} = 510 nm) is produced by the recombination of two radicals with hydrolysis.[117] Vanadium(IV) produced is oxidized

by bromate and thus returns in the cyclic reaction.

In this study, *p*-anisidine was employed as substrate for the vanadium-catalyzed reaction. According to the obtained absorption spectra as shown in Fig. 4-3, the catalytic oxidation of *p*-anisidine can proceed by similar homolytic mechanism mentioned above. Therefore, it was concluded that the most probable product in this study was *N*-(4-methoxyphenyl)-quinoneimine:

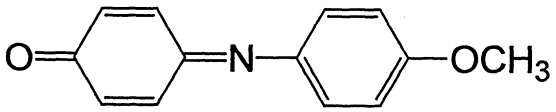

4.3.2. Design of touchscreen programmable controller for SIDL-FA

It is self-evident that sophisticated flow-based analyses have been developed by automatic controls of gas and/or liquid handling devices such as pumps and valves. Although it is easy for advanced users to accomplish such controls, a user-friendly ubiquitous control system is still required to have flow-based analyses widespread. As mentioned in Experimental section, the proposed TSC (Fig. 4-4) controls three pumps (ON/OFF), port selection of V_1, valve switching of V_2 and V_3 and a recorder. As can be seen in Fig. 4(c), one can start analysis with a touch on the screen panel which displays the current states of three valves and three pumps in real time. Also, the analytical protocol can be easily modified by touching to "CONFIG." on the display area.

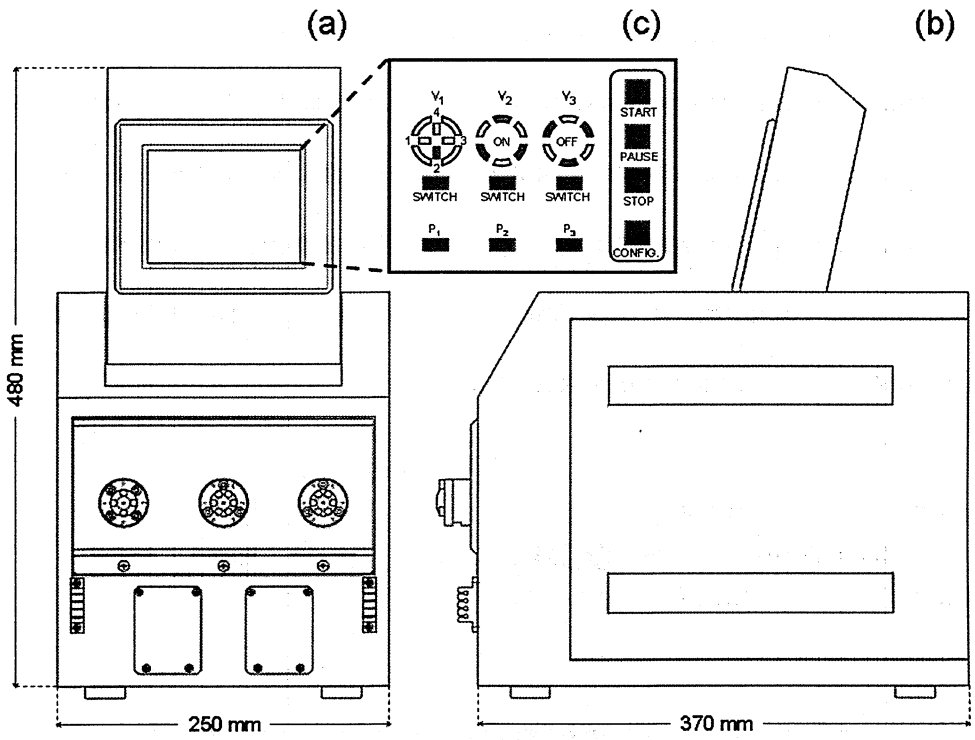

Fig. 4-4 Touchscreen controller.

(a), front view; (b), side view; (c), example of indication on the touchscreen panel.

4.3.3. Optimization

The protocol depicted in Table 4-1 was temporarily modified in the optimization study. In this study, the first loop (L_1) shown in Fig 4-1 was not used therefore the optimization was carried out by measuring the absorbance of the uncatalyzed and catalyzed reaction products from only the second loop (L_2).

4.3.3.1. Effect of stopping time in loop

Stopping time in L_2 was varied from 2 to 5 min. The symbols in Fig. 4-5 denote

absorbance values of uncatalyzed (○), catalyzed (□) and the net (Δ). The uncatalyzed reaction was little affected by an increase in stopping time. The catalyzed reaction, on the contrary, was dramatically enhanced. Taking into account sample throughput, a stopping time of 3 min was chosen.

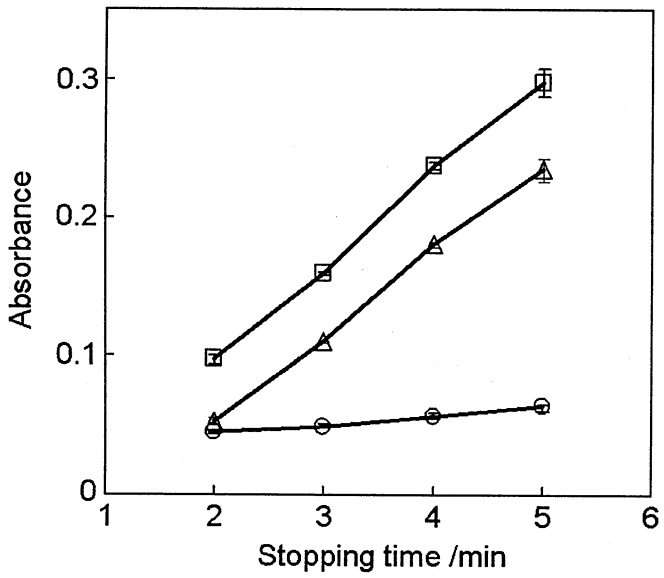

Fig. 4-5 Effects of stopping time in L_2 on uncatalyzed (○) and catalyzed (□) reactions. (Δ), net absorbance; C_V, 1.0 μg L^{-1}. Other conditions as in Fig. 4-1.

4.3.3.2. Effect of temperature

Temperature setting of the PID controller was varied from 80 to 105°C. The absorbance of uncatalyzed reaction was constant in this temperature range. The response of catalyzed reaction increased with raising temperature. At higher temperatures than 105°C, we encountered bubble-induced detector problems. A temperature setting of 105°C was therefore chosen.

4.3.3.3. Effect of pH

Fig. 4-6 shows the effect of pH on the responses. The x-axis of Fig. 4-6 stands for pH of the waste solution. The response of catalyzed reaction had a pseudoplateau in the range of 2.7 – 3.0, and the response of uncatalyzed reaction slightly decreased in the examined pH range. Although the net absorbance was highest at pH 2.7, we chose a reaction pH of 3.0, because the blank response at pH 3.0 was a little bit lower than that at pH 2.7. The pH value of RS_1 containing acetate buffer was adjusted at pH 3.3 to obtain the chosen pH 3.0 for the waste solution.

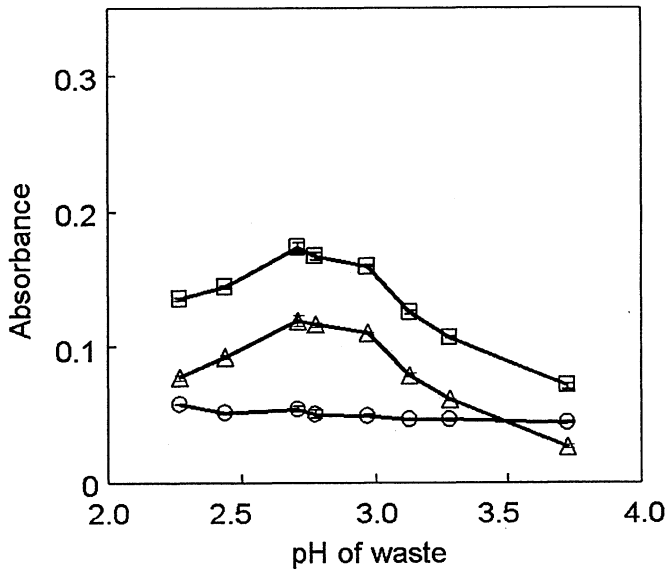

Fig. 4-6 Effects of pH on uncatalyzed (○) and catalyzed (□) reactions. (Δ), net absorbance; C_V, 1.0 μg L^{-1}. Other conditions as in Fig. 4-1.

4.3.3.4. Effect of p-anisidine concentration

The effect of *p*-anisidine concentration on the responses was studied over the range from 40 to 90 mM in RS_1. The response of catalyzed reaction increased monotonically with *p*-anisidine concentration, but that of uncatalyzed reaction also increased slightly. Hence, *p*-anisidine concentration of 80 mM was chosen.

4.3.3.5. Effect of bromate concentration

Both catalyzed and uncatalyzed reactions accelerated with increasing bromate concentration over the range from 10 to 200 mM. Taking into consideration the blank response, a bromate concentration of 50 mM was chosen.

4.3.3.6. Effect of Tiron concentration

The use of properly selected activators for catalytic reactions offers an improvement in the sensitivity and/or the selectivity.[118] There have been numerous reports on vanadium-catalyzed indicator reactions in which some ligands acted as activators: oxine,[119] oxalic, citric[120] and sulfosalicylic acids,[104,120] Tiron,[96,101,105] tartrate,[97] gallic acid[103] and hydrogen carbonate.[107] We employed Tiron as the activator for the proposed catalytic oxidation of *p*-anisidine. The effect of Tiron concentration on the responses was shown in Fig. 4-7. The response of catalyzed reaction remained almost constant at Tiron concentrations higher than 0.1 M. The net value was highest at 0.15 M, so this concentration was chosen.

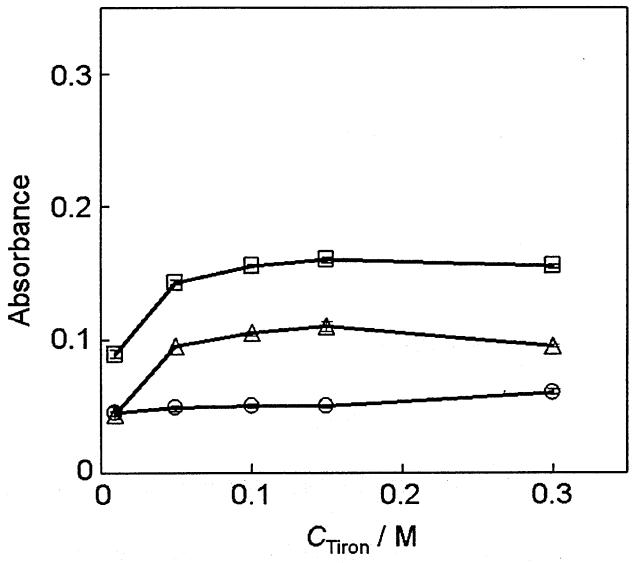

Fig. 4-7 Effects of Tiron concentration on uncatalyzed (○) and catalyzed (□) reactions. (Δ), net absorbance; C_V, 1.0 μg L^{-1}. Other conditions as in Fig. 4-1.

Bontschev[118] reported that hydroxy acids, such as oxalic, citric and gallic acids, acted as activator for vanadium-catalyzed oxidation of *p*-phenetidine by chlorate. Such activators (A) are oxidized easily by vanadium(V) to radicals (A·),

$$V(V) + A \rightarrow \quad A\cdot + V(IV) \qquad (2)$$

which then react with the coexisted *p*-phenetidine (S) to produce its radical (S·),

$$A\cdot + S \rightarrow \quad A\,(\text{or } A') + S\cdot \qquad (3)$$

followed by the recombination of S· as described in the section 4.3.1. Tiron has two hydroxyl groups to be easily reduced. Hence the similar pathway as mentioned above

can be thought to proceed in the present catalytic reaction, although there are several possible mechanisms.

4.3.4. Analytical characteristics

The typical system output is shown in Fig. 4-8. As described in the section 4.2.3., the SIDL-FA protocol depicted in Table 4-1 gave two peaks for two loops; for example (a) and (a') in Fig. 4-8 are of peaks for uncatalyzed reaction obtained from L_1 and L_2, and (b) and (b') are of peaks for 1 μg L^{-1} vanadium from L_1 and L_2. As can be seen in Fig. 4-8, a negative peak was observed in each measurement. This is probably due to the

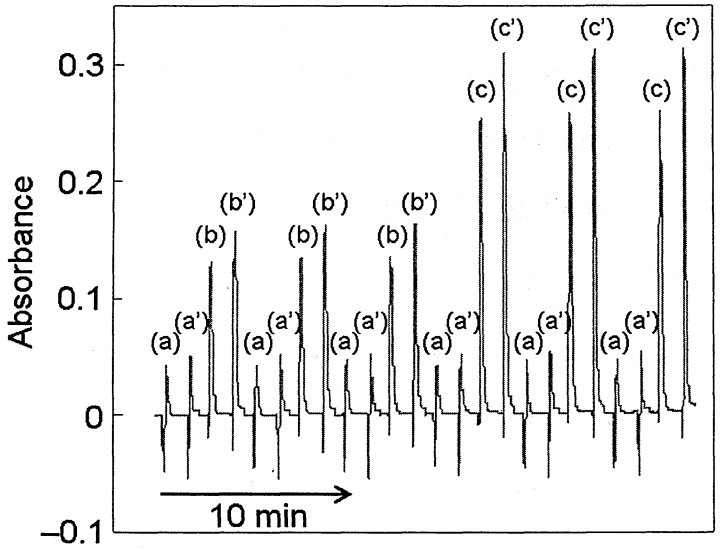

Fig. 4-8 Typical system output for response to standard vanadium(V) obtained from L_1 ((a), (b) and (c)) and L_2 ((a'), (b') and (c')).

C_V in μg L^{-1}: (a) and (a'), 0; (b) and (b'), 1.0; (c) and (c'), 2.0. Other conditions as in Fig. 4-1. The abscissa does not stand for the total analysis time, but stands for the data acquisition time (steps 6–8, see Table 4-1).

differences in refractive indices between the resulting solution from each loop and the carrier stream (10 mM nitric acid). These negative peaks due to Schlieren effect could be neglected in this system because acceptable calibration curves for L_1 and L_2 in the range of 0 – 2.0 μg L^{-1} vanadium(V) were obtained from only positive peaks without any compensation:

Net absorbance = 0.104[V(V), μg L^{-1}] – 0.00504

for L_1 (r^2 = 0.993) (4)

Net absorbance = 0.128[V(V), μg L^{-1}] – 0.00678

for L_2 (r^2 = 0.993) (5)

The lower slope value of L_1 was caused by the longer distance between L_1 and the detector than that for L_2. However, the 3σ limit of detection for L_1 (0.038 μg L^{-1}) was comparable to that for L_2 (0.037 μg L^{-1}). Therefore, analytical values of two unknown samples using L_1 and L_2 can be obtained within 370 s. The sample throughput is therefore approximately 20 samples h^{-1}. In the previous study on SIL-FA with a single loop,[8] 280 s was needed to obtain an analytical value of one unknown sample (the sample throughput was approximately 13 sample h^{-1}). The proposed SIDL-FA with two loops is superior in sample throughput. The R.S.D. values (n = 5) in the present study were 0.81 (L_1) and 1.1% (L_2) for responses at 1.0 μg L^{-1}.

4.3.5. Interference study

The effects of various foreign ions on the response of 1.0 μg L^{-1} vanadium(V)

obtained from L_2 were studied. The results are summarized in Table 4-2. The tolerance limit was defined as the interference that yielded a relative error less than or equal to ±5%. Among the tested foreign ions, iron(III) gave the largest positive interference. In our previous paper,[121] the oxidation of *p*-anisidine by hydrogen peroxide was catalyzed by iron. Hence iron(III) may act as a catalyst for the oxidation reaction in this study. Since 50 μg L^{-1} iron(III) is tolerable for the determination of 1.0 μg L^{-1} vanadium(V) by the proposed method, the applicability of this method to natural water analysis would be limited by this value. It was reported that 40 – 80 μg L^{-1} iron existed in well water.[122] However, the proposed method is allowed to be applied to vanadium-rich water analysis.

Table 4-2 Tolerance limits of foreign ions on the determination of 1.0 μg L^{-1} vanadium(V).

Tolerance limit / μg L^{-1}	Ion added
50000	Mg(II), Na(I), Ca(II), Cd(II), K(I), Rb(I), Cl^-, Br^-, F^-, NO_3^-, SO_4^{2-}
20000	Ni(II), Mn(II), Pb(II)
10000	Zn(II), Sn(IV)
5000	Se(IV)
2000	Al(III), Co(II), Si(IV)
500	Ti(IV)
200	Cr(VI)
100	Cu(II)
50	Fe(III)

4.3.6. Application

The proposed SIDL-FA method was applied to the determination of vanadium in

commercial bottled water samples (Table 4-3). A paired *t* test was performed on the data obtained by the proposed method and ICP-MS. The experimental *t* value was 1.538 which is less than the critical *t* value at the 95% confidence level for three degrees of freedom (3.182). The statistical analysis revealed that there is no significant difference between the two methods. In addition, the analytical values were in fair agreement with the labeled values.

Table 4-3 Determination of vanadium in bottled mineral water.

Sample	Found / μg L^{-1}			Labeled / μg L^{-1}
	Proposed		ICP-MS	
	Loop 1	Loop 2		
1[a]	92±0.9	–	92±1.7	91
2[b]	–	50±0.4	49±0.6	50
3[b]	62±1.5	–	60±4.0	62
4[c]	–	0.97±0.3	$1.0\pm0.0_5$	1

[a] The water was diluted to 200 times with 10 mM nitric acid before measurement.
[b] The water was diluted to 100 times with 10 mM nitric acid before measurement.
[c] The water was diluted to 2 times with 10 mM nitric acid before measurement.

4.4. Conclusion

An automated SIDL-FA system have been proposed here for kinetic-catalytic determination of vanadium in bottled drinking water. The designed touchscreen controller could successfully perform the SIDL-FA operation sequence. The SIDL-FA technique provides smaller reagent consumption than conventional FIA system. Such automated SIDL-FA technique is expected to be applicable to the other kinetic-catalytic methods of analysis.

Chapter 5 Highly Sensitive Determination of Cadmium and Lead in Leached Solutions from Ceramic Ware by Graphite Furnace Atomic Absorption Spectrometry Coupled with Sequential Injection-Based Solid Phase Extraction Method[123]

5.1. Introduction

FIA is a useful technology for the automation and the simplification of analysis processes. In recent years, analytical techniques for ultra trace elements in environmental, industrial and biological samples have been often required. Since Olsen *et al.*[124] proposed on-line solid-phase extraction (SPE) coupled with FIA, several techniques using SPE, such as ion-exchange resins, chelating resins, and hydrophobic materials, have been applied to the enrichment of analytes and the removal of interfering substances and matrix.[125,126]

For the trace determination of heavy metals, spectrophotometry, fluorimetry and flame atomic absorption spectrometry (FAAS) coupled with on-line sample pre-treatment methods are very useful and convenient because of easy assembly and hyphenation. For example, Q Sepharose FF (anion-exchange resin) was used to detect hexacyanoferrate(II) with 1,10-phen and spectrophotometry.[127] The formation of boron complex with 1,8-dihydroxy-3,6-naphthalenesulphoric acid and small column packed with Sephadex G-25 gel was used for sensitive determination of boron by fluorescence detection.[128] In addition, simultaneous determination of silicate, phosphate, and arsenate utilizing anion-exchange column (TSK-gel SAX) and heteropoly blue was reported.[129] Flow injection (FI)-spectrophotometry for the speciation of Cr(VI) and Cr(III) using diphenylcarbazide and C_{18} column was also reported.[130] For lead and cadmium

determination, the complex formation with 2-(5-nitro-2-pyridylazo)-5-(*N*-propyl-*N*-sulfopropylamino)phenol and FI-ion chromatography systems were used; the detection limits were 4.8 μg L^{-1} for lead and 1.9 μg L^{-1} for cadmium.[131] Spectrophotometry gives lower running cost. However, sensitivity is not sufficient for trace analysis.

To enhance selectivity and sensitivity for metal determination, FAAS with SPE was proposed for trace lead determination in high purity metals: the detection limit of lead by normal FAAS is about 10 μg L^{-1}. FI-on-line preconcentration and separation of lead using a Pb-selective chromatographic resin (Pb-Spec™) were utilized for reducing the risk of contamination from the laboratory environment[24,132] where lead eluted was simply introduced into the nebulizer. In other FAAS methods, after adsorption of non-charged lead-PDC (pyrrolidine dithiocarbamate) complex on the hydrophobic PTFE material, the complex eluted with isobutyl methyl ketone was introduced into the nebulizer; the sampling rate was 15 h^{-1}, and the detection limit was 0.8 μg L^{-1}.[133] Dadfarnia *et al.*[134] have reported the determination of lead using FI-FAAS with fibrous alumina.

Later, for a highly sensitive method, electrothermal atomic absorption spectrometry (ETAAS) with FI-SPE was carried out, because ETAAS is more sensitive compared with FAAS (*ca.* 10-fold). Sperling *et al.*[135] proposed the interface of the FI system to the graphite furnace by connecting the transfer capillary of the FI system to the sample introduction capillary of the autosampler arm. Hirano *et al.*[32] have proposed FI-GFAAS (graphite furnace atomic absorption spectrometry) with a minicolumn packed with Muromac A-1 for the determination of trace cadmium. Nakajima *et al.*[35] have reported the determination of lead by coprecipitation with iron(III) hydroxide and SPE with Pb-Spec™ utilizing FI-ETAAS. The methods mentioned above were applied to the

determination of cadmium and lead in water samples. However, in FI system, it leads to continuous reagents consumption and therefore, a large amount of waste generation.

SIA proposed by Ruzicka *et al.* in 1990 has several advantages in the automation and miniaturization of analytical methods. In SIA, small amounts of the sample and reagent zones are sequentially aspirated into the holding coil and therefore, it is possible to reduce considerably the reagent consumption compared with FIA system. On-line sample-pre-treatment schemes for trace-level determination of metals by coupling FI and/or SI with ICP-MS[136] and SIA for on-line sample-handling and pre-treatment[137] were reviewed. In general, SIA with sample pre-treatment is fully automated. The aspirated sample is transferred to the column for the separation and the concentration of the analyte; the retained analyte can be eluted using an adequate eluent.

SIA with bead injection and lab-on-valve (SI-BI-LOV) was proposed for the determination of lead using Sephadex G-25 impregnated by dithizone by ETAAS[34]: the detection limit was 0.3 ng and the sample throughput was 12 h^{-1}. In that system, the beads were directly propelled into a graphite tube. Long *et al.*[36] used poly(styrene-divinyl-benzene) beads containing octadecyl moieties (C_{18}-PS/DVB) as reagent carriers. In this SI-BI-LOV system, 1,5-diphenylcarbazide-loaded C_{18}-PS/DVB beads were used for the preconcentration of chromium(VI).

Nowadays, people notice a great interest in food safety. Especially, there are several social problems; foods and rice contaminated with agricultural chemicals and heavy metals were widely distributed. Furthermore, it has been reported that heavy metals were leached from some earthen ware pot. It is very important to determine toxic metals at sub-ppb levels for removing anxiety and improving safety. In 2008, the Government of Japan notified that cadmium and lead leaching from glassware, ceramic ware, and hollowware into foodstuff should be strictly controlled (the Ministry of Health, Labour,

and Welfare Notification No. 416, 2008). There have been only a few reports on the determination of cadmium and lead in ceramic ware leaching solutions by GFAAS so far.[138,139] Recently, a method has been developed for the determination of lead in a ceramic ware leaching solution by FI on-line preconcentration using Pb-Spec™ and spectrophotometric detection.[10] However, lead was not found in the leaching solutions, because its concentrations were lower than the limit of quantitation.

In this paper, an SI-based automated on-line sample pretreatment system coupled to GFAAS (Auto-Pret-GFAAS system) was developed for the determination of trace cadmium and lead leached from ceramic ware. The Auto-Pret-GFAAS system was used as a SPE pretreatment with a handmade minicolumn packed with chelating resin. It is discussed that the analytical characteristics of the proposed fully automated system that can be useful for the analysis of cadmium and lead at sub-ppb levels in solutions leached from ceramic ware and tap water.

5.2. Experimental

5.2.1. Apparatus

A polarized Zeeman atomic absorption spectrophotometer (Z-2700, Hitachi High-Technologies, Tokyo) with pyrolytically coated graphite furnace was used for the detection of cadmium and lead. The operating conditions of GFAAS are shown in Table 5-1. Fig. 5-1 shows the diagram of Auto-pret-GFAAS system used in this work. This system consists of a glass syringe pump with a volume of 12.5 mL syringe (Hamilton PSD/4 pump module), an eight-port selection valve and a six-way switching valve (Hamilton). A minicolumn for the preconcentration was prepared by packing 20 mg of

chelating resin, NOBIAS CHELATE-PA1 (Hitachi High-Tech Fielding, Tokyo), into a PTFE tubing (i.d. 3 mm). The both ends of the column were plugged with cotton. The handmade minicolumn containing a chelating resin was set on the six-way switching valve. All protocol for SPE was controlled by home-made software (Visual Basic) installed in a personal computer. A trigger switch was placed at aside of the graphite furnace. The trigger was turned on by the movement of the autosampler arm of the GFAAS, so that the SI-based SPE system can be synchronized with GFAAS.

Table 5-1 Operating parameter of GFAAS.

	Cd			
	Temperature / °C	Ramp / sec	Hold / sec	Flow rate of Ar / mL / min
Drying	80 – 140	100	–	200
Ashing	300	–	20	200
Atomization	1500	–	5	30
Clean-out	1800	–	4	200
Wavelengh			228.8 nm	
Lamp current			7.5 mA	
Slit width			1.3 nm	
Measurement mode			Peak height	
	Pb			
	Temperature / °C	Ramp / sec	Hold / sec	Flow rate of Ar / mL / min
Drying	80 – 140	100	–	200
Ashing	400	–	20	200
Atomization	2000	–	5	30
Clean-out	2200	–	4	200
Wavelengh			283.3 nm	
Lamp current			7.5 mA	
Slit width			1.3 nm	
Measurement mode			Peak height	

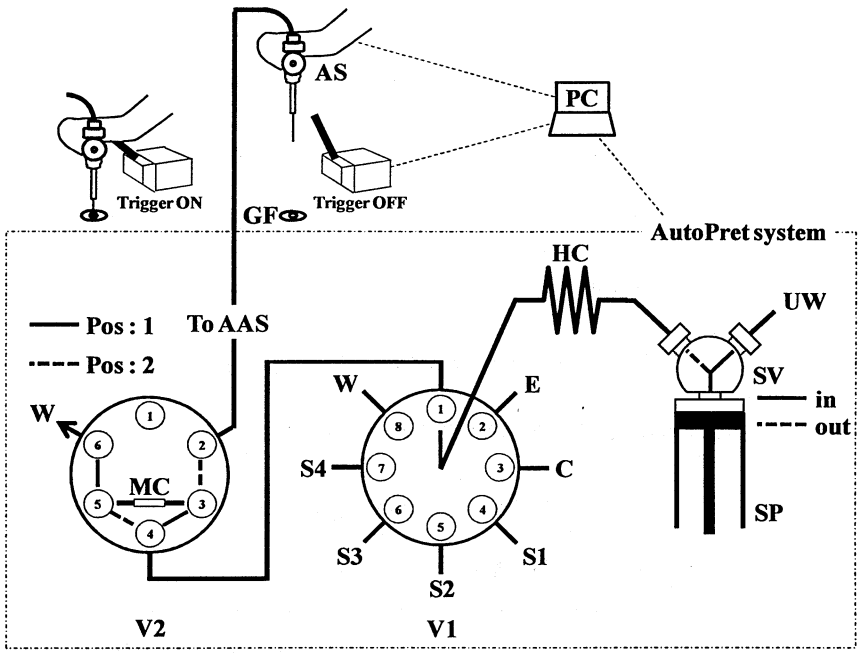

Fig. 5-1 Schematic diagram of the automated pretreatment system for GFAAS (Auto-Pret-GFAAS system).

AS, autosampler arm of GFAAS; GF, graphite furnace; SV, Syringe Valve; SP, Syringe pump; V1, Eight-port selection valve; V2, Six-way switching valve; MC, Minicolumn; HC, Holding coil; UW, Ultrapure water; E, Eluent (3M nitric acid); C, Column conditioner; S1,S2,S3,S4, Sample or standard; W, Waste.

5.2.2. Reagents

Ultrapure water obtained by an Elix 3/Milli-Q Element System (Nihon Millipore, Tokyo) was used throughout all experiments. A 0.1 M ammonium acetate solution was prepared by dissolving ammonium acetate (≧97.0 %, analytical grade, Sigma-Aldrich Japan, Tokyo) in water and adjusted to pH 6 with 10 % nitric acid. After adjusting pH, the solution was passed through a column (CHELATE-PA1F, Hitachi High-Tech Fielding) for removing heavy metal impurities in it. Stock solutions of cadmium and

lead (10 mg L^{-1}) were prepared by diluting 1000 mg L^{-1} standard solutions for AAS (Wako Pure Chemical Industries, Osaka) with 0.1 M nitric acid prepared from concentrated nitric acid (60 %, ultrapure reagent, KANTO CHEMICAL, Tokyo). Working solutions of cadmium and lead were diluted with 0.1 M ammonium acetate adjusted to pH 6. The eluent was 3 M nitric acid solution prepared from concentrated nitric acid (60 %, analytical grade, Sigma-Aldrich Japan, Tokyo). 4% acetic acid solution to extract cadmium and lead from ceramic ware was prepared from acetic acid (≧99.7 %, analytical grade, Sigma-Aldrich Japan).

5.2.3. Tap water sample

Tap water taken at our laboratory (Aichi Institute of Technology) was filtered through the membrane filter (mixed cellulose ester, 0.45 μm, Advantec, Toyo Roshi Kaisha, Japan). After filtration, 1 mL of it was diluted with 5 mL of 0.2 M ammonium acetate adjusted to pH 6 and 4 mL of water.

5.2.4. Extraction from ceramic ware

Ceramic ware was filled with 4% acetic acid solution and kept in the dark for 24 hours. After extraction, the extract was adjusted to pH 6 using ammonia solution (28 – 30 %, analytical grade, Merck, Germany).

5.2.5. Preconcentration procedure

The protocol for the preconcentration of cadmium and lead is shown in Table 5-2.

Table 5-2 Protocol for the preconcentration of cadmium and lead (1 mL of sample).

Protocol	Remark
Repeat: 3 times	
S1.Syringe Valve: "OUT" V2.Valve Pos: 1 V1.Valve Pos: 3 S1.Aspirate: 500 µL | Speed: 250 µL/s V1.Valve Pos: 1 S1. Dispense: 500 µL | Speed: 50 µL/s	Conditioning the minicolumn
V1.Valve Pos: 4 S1.Aspirate: 1000 µL | Speed: 250 µL/s V1.Valve Pos: 1 S1. Dispense: 1000 µL | Speed: 180 µL/s	Loading the sample into the minicolumn
S1.Syringe Valve: "IN" S1. Aspirate: 500 µL | Speed: 250 µL/s S1.Syringe Valve: "OUT" V1.Valve Pos: 1 S1. Dispense : 500 µL | Speed: 50 µL/s	Removing the matrix in the minicolumn
V2.Valve Pos: 2 V1.Valve Pos: 2 S1.Aspirate: 1000 µL | Speed: 250 µL/s S1.Syringe Valve: "IN" S1. Aspirate: 1000 µL | Speed: 250 µL/s	Aspiration of eluent and water for cleaning the column
V1.Valve Pos: 1 S1.Syringe Valve: "OUT" S1.Dispense: 410 µL | Speed: 180 µL/s	Eluting the collected sample in the column and transportation of eluted sample to the edge of the nozzle
Wait for "ON" signal Delay: 1 s S1.Dispense: 50 µL | Speed: 10 µL/s Delay: 9 s	Injection of the eluted sample into the graphite furnace
S1. Dispense: 1540 µL | Speed: 50 µL/s	Cleaning the minicolumn
Loop;	

First, column conditioning is carried out: 500 μL of 0.1 M ammonium acetate adjusted to pH 6 is aspirated via the port 3 of V1, and then dispensed through the port 1 of V1. After conditioning the column, 1000 μL of the sample solution is aspirated via the port 4 of V1 (when a 10 mL of sample was introduced, it is aspirated at 500 μL sec^{-1}), and then dispensed through the port 1 of V1 for preconcentration. After the sample is loaded into the column, washing the column is carried out using ultrapure water. Next, 1000 μL of 3 M nitric acid is aspirated into the holding coil and 1000 μL of ultrapure water is aspirated into the syringe. And then, the switching valve turns another position and 410 μL of the eluent is dispensed through the port 1 of V1 for eluting collected sample in the column and transportation of eluted sample to the edge of the nozzle. After transportation, the autosampler of GFAAS goes down into the graphite furnace and presses a trigger switch placed at aside of the furnace. Once the switch is pressed, 50 μL of the eluted sample is introduced into the furnace. And then washing the column is carried out and preconcentration for a next sample is carried out.

5.3. Results and Discussion

5.3.1. Auto-pretreatment system coupled to GFAAS

Sabarudin *et al.* [16] developed an automated SI-based on-line preconcentration system with ICP-AES detection (Auto-Pret-AES) for the determination of lead. A lead-selective resin, Analig Pb-01, was packed in a minicolumn and installed into the Auto-Pret-AES system. An Auto-Pret AES system equipped with a Muromac A-1 packed minicolumn has also been applied to the determination of 13 trace metals in natural water samples.[17] In this study, an Auto-Pret- GFAAS system has been proposed.

In this study, the Auto-Pret-GFAAS system equipped with a NOBIAS CHELATE-PA1 minicolumn was automatically controlled by laboratory-built software (Visual Basic) installed in a computer, while the GFAAS including an autosampler arm was operated by a built-in-software installed in the same computer. In order to synchronize these two software programs, a trigger switch was employed. As can be seen in Fig. 5-1, the autosampler arm presses the trigger, and then immediately the Auto-Pret-GFAAS system introduces a 50 μL standard/sample solution into the graphite furnace. This Auto-Pret-GFAAS system can be attached with any commercially available GFAAS instruments with an autosampler arm.

5.3.2. Optimization study

The optimization of the Auto-Pret-GFAAS system was carried out using 100 ng L^{-1} of cadmium and 1 μg L^{-1} of lead.

5.3.2.1. Effect of eluent volume

In the SI-based SPE system, eluent volume is an important parameter for the sensitivity because an eluted sample is dispensed toward the edge of the nozzle by an eluent solution before introduction to the graphite furnace. Too small eluent volume will result in lowered sensitivity because an eluted sample does not reach to the edge. Conversely, too large eluent volume will also result in lowered sensitivity because the eluted sample will be discharged to waste before measurement. In this study, the effects of dispensing volume of the eluent with different conditions on absorbance of cadmium and lead were investigated. Firstly, four columns with different inner diameters (i.d.)

ranged from 2 to 5 mm were tested at a constant eluent (nitric acid) concentration of 3 M. Same amount of chelating resin (20 mg each) was packed into each minicolumn, and therefore the lengths of the chelating resin columns with inside 2, 3, 4, and 5 i.d. were 18.9, 8.2, 4.6, and 2.9 mm, respectively. The results are shown in Fig. 5-2.

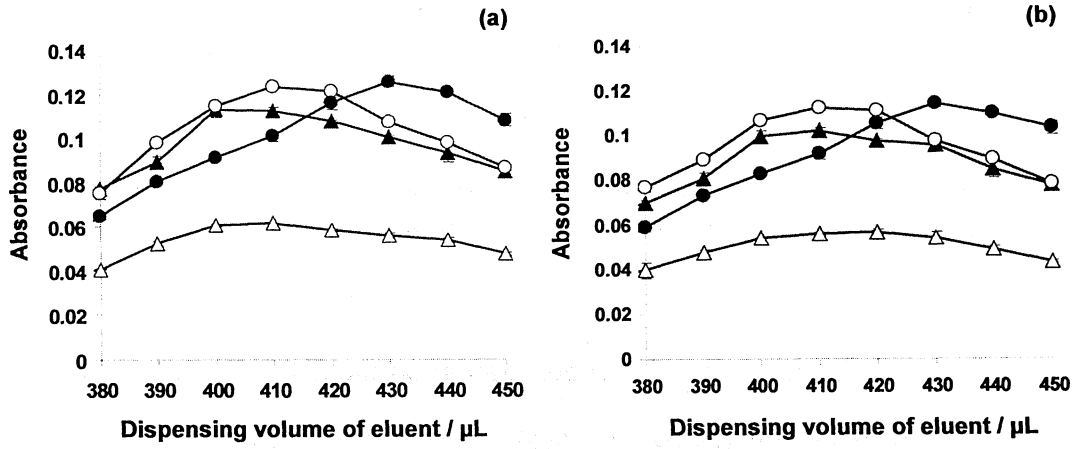

Fig. 5-2 Effects of inner diameter of minicolumn on the determinations of (a) 100 ng L^{-1} cadmium and (b) 1 µg L^{-1} lead.
Inner diameter (mm): (●), 2; (○), 3; (▲), 4; (Δ), 5.

Columns with 2 and/or 3 mm i.d. gave the highest sensitivities for both analytes. However, a 2 mm i.d. column needed larger eluent volume to obtain the highest sensitivity, probably because it was hard for both metals to be eluted from the longest column. The column with 5 mm i.d. gave lower sensitivity because of dispersion. In this study, a 3 mm i.d. column was chosen because it gave a faster sample throughput than that of a 2 mm i.d. column. Secondly, the concentration of nitric acid for elution was varied from 1 to 4 M. As can be seen in Fig. 5-3, 3 and 4 M nitric acid gave the highest sensitivity for both analytes. A 3 M nitric acid was chosen as eluent because higher acid

concentration would damage a graphite furnace.

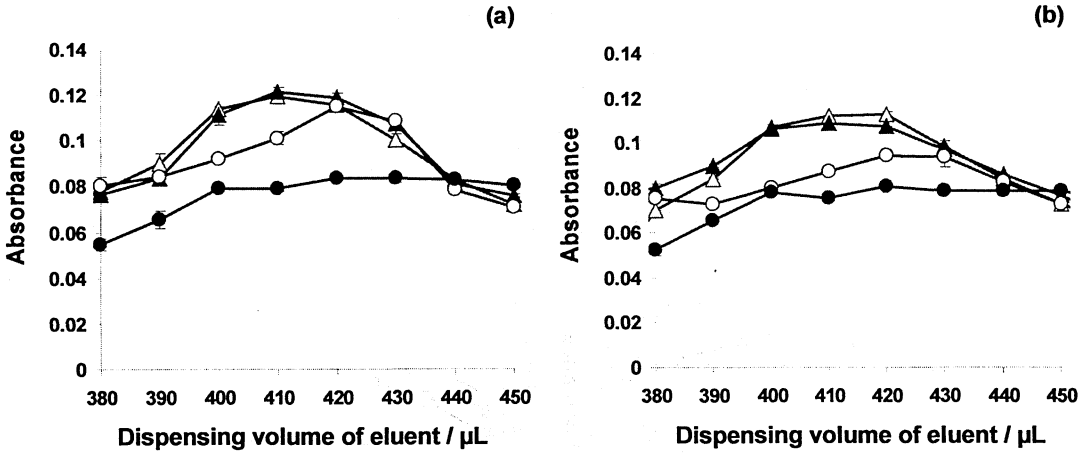

Fig. 5-3 Effects of eluent (nitric acid) concentration on the determinations of (a) 100 ng L^{-1} cadmium and (b) 1 µg L^{-1} lead.
Nitric acid concentration (M): (●), 1; (○), 2; (▲), 3; (Δ), 4.

5.3.2.2. Effect of pH

Sample pH affects adsorption metal ions on chelating resin. Therefore the effect of pH on the preconcentration for cadmium and lead was studied. The pH of the sample and column conditioner was adjusted from 3 to 9 by adding 10 % nitric acid or 10 % ammonia solution to 0.1 M ammonium acetate. The results are shown in Fig. 5-4. On the cadmium determination, the absorbance increased with an increase pH up to 5. At pH above 5, while the sensitivity was constant. On the lead determination, the highest sensitivity was obtained at pH from 4 to 7, and the absorbance drastically decreased at pH higher than 7. Sakamoto *et al.*[140] reported similar result for lead with the same chelating resin. The absorbance decrease may be due to the formation of lead (II)

hydroxide. Consequently, the pH of the sample and column conditioner was adjusted at 6.

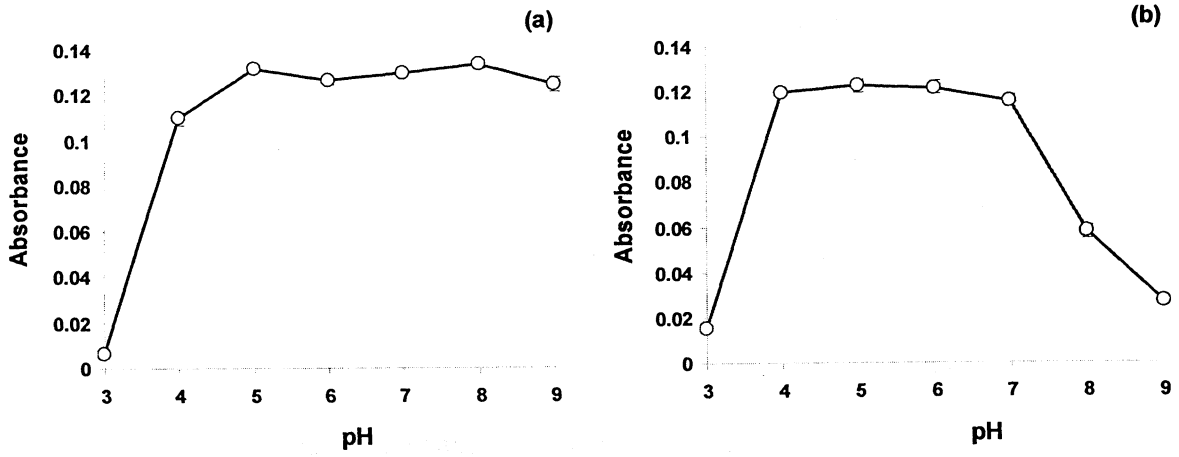

Fig. 5-4 Effects of pH on the preconcentration for (a) 100 ng L^{-1} cadmium and (b) 1 μg L^{-1} lead.

5.3.2.3. Effect of other variables

The effect of loading and eluting flow rates was examined in the range of 20 – 180 μL sec^{-1}. Both flow rates did not have any appreciable effects on the absorbance. Since the faster flow rate provides the shorter analysis time, a flow rate of 180 μL sec^{-1} was selected for loading and eluting. Injection volume of eluted sample into the graphite furnace was investigated. Injection volume of a 100 μL gave higher sensitivity compared to that using 50 μL of injection volume, but the lifetime of the graphite furnace was about 80 times-use in the case of 100 μL. On the other hand, it became about 230 times-use when the injection volume was 50 μL. In addition, the time for drying in the GFAAS analysis is 50 seconds shorter than that of the 100 μL injection

volume. Taking into consideration the lifetime of the graphite furnace and analysis time, 50 μL of injection volume into the graphite furnace was chosen.

5.3.3. Analytical characteristics

As mentioned above, the detection limits by Sperling *et al.*[135] were 0.8 ng L^{-1} for cadmium and 6.5 ng L^{-1} for lead with 22 h^{-1} measurements. In the Muromac A-1 column-FI-GFAAS system, the detection limit for cadmium was 0.2 ng L^{-1}.[32] Table 5-3 shows the analytical characteristics of the proposed system under the optimum conditions. When a sample volume was 1 mL, the limits of detection (3σ) were 0.20 ng L^{-1} for cadmium and 2.6 ng L^{-1} for lead, and the limits of quantitation (10σ) for cadmium and lead were 0.66 ng L^{-1} and 8.8 ng L^{-1}, respectively. The enrichment factor calculated from the ratio of a slope of the calibration curve with preconcentration to that without preconcentration were 7.98 for cadmium and 7.48 for lead. The sample throughput was about 47 h^{-1}. When a 10 mL of sample was used, the sensitivity was approximate 10 times as high as that using 1 mL of sample. However, the sample throughput was about 21 h^{-1} because a longer time for preconcentration was required. The lifetime of the minicolumn was fairly long. We could use the same column at least 2000 times measurements. The proposed system has big advantages in sensitivity, rapidity and simplicity over the conventional ones.

Table 5-3 Analytical characteristics on the proposed system.

Analytical parameters				
	Cd		Pb	
Sample volume / mL	1	10	1	10
Linear range	1 – 200 ng L^{-1}	0.1 – 20 ng L^{-1}	0.1 – 2 μg L^{-1}	0.01–0.2 μg L^{-1}
Slope	0.00125	0.0116	0.0924	0.977
Correlation coefficient	0.999	0.998	0.999	0.996
LOD[a] / ng L^{-1}	0.197	0.0231	2.63	0.630
LOQ[b] / ng L^{-1}	0.656	0.0772	8.77	2.10
RSD[c] / % (n = 10)	2.61 (100 ng L^{-1})	2.27 (10 ng L^{-1})	3.00 (1μg L^{-1})	2.09(0.1μg L^{-1})
Enrichment factor	7.98	69.0	7.48	76.3

a. Limit of detection

b. Limit of quantitation

c. Relative standard deviation

5.3.4. Interference study

The chelating resin used in this work can separate alkaline and alkali-earth metals from the sample solution. But other heavy metals are trapped on the resin. Therefore, the effect of heavy metals on the determination of 100 ng L^{-1} cadmium and 1 μg L^{-1} lead were examined. The results are shown in Table 4. An error of less than 5% was considered to be tolerable on the absorbance. Any other metals tested did not interfere on the determination of cadmium and lead.

Table 5-4 Interference of foreign ions on the determination of 100 ng L^{-1} cadmium and 1 μg L^{-1} lead

Tolerance limit / mg L^{-1}	Cd determination	Pb determination
10	Cr (VI)	
1	B (III), Al (III), Fe (III)	Cr (VI), Zn (II), Cd (II)
0.5	Zn (II), Pb (II)	B (III), Al (III)
0.1		Fe (III)

5.3.5. Application

The proposed method was applied to the determination of cadmium and lead in tap water and in leached solutions from ceramic ware using 4% acetic acid for 24 h at room temperature (dark room). General procedure is as follows.[141] Evaporate 20 mL of the solution leached from the ceramic ware to dryness and add 2 mL of 6 M hydrochloric acid and evaporate it again. After dissolving the residue with 0.1 M nitric acid, dilute with ultrapure water to 10 mL. The metal ions leached are usually measured using atomic absorption spectrometer. However, the procedure is time-consuming and tedious. Accordingly, highly sensitive and selective analytical method with Auto-Pret-GFAAS system was applied for preconcentration and direct measurement without evaporation. The analytical values were obtained by calibration curve method. The recovery tests were also carried out. The results are summarized in Table 5-5. Cadmium concentration in the extracts was 0.820 – 1.38 ng L^{-1} and that of lead was 0.307—2.26 μg L^{-1} by the proposed method. The recovery for cadmium and lead was 93.9 – 105 %.

Table 5-5 Determination of cadmium and lead in the tap water and the extract from ceramic ware.

Cd	Added / ng L^{-1}	Found[a] / ng L^{-1}	Recovery / %	In sample / ng L^{-1}	ICP-MS method / ng L^{-1}
Tap water[b]	0	14.4		144±4	147±3
	50	65.6	102		
	100	114	99.6		
Extract 1	0	1.31		1.38±0.06	n.d.[c]
	50	52.5	102		
	100	100	98.7		
Extract 2	0	1.00		1.06±0.13	n.d.
	50	50.6	98.9		
	100	101	99.2		
Extract 3	0	0.779		0.820±0.061	n.d.
	50	50.1	98.4		
	100	96.4	95.4		
Pb	Added / μg L^{-1}	Found[a] / μg L^{-1}	Recovery / %	In sample / μg L^{-1}	ICP-MS method / μg L^{-1}
Tap water[b]	0	0.222		2.22±0.36	2.20±0.03
	0.5	0.748	105		
	1.0	1.21	98.8		
Extract 1[b]	0	0.214		2.26±0.02	1.92±0.02
	0.5	0.736	105		
	1.0	1.23	102		
Extract 2	0	0.642		0.677±0.030	0.580±0.006
	0.5	1.11	95.0		
	1.0	1.58	93.9		
Extract 3	0	0.292		0.307±0.003	0.282±0.002
	0.5	0.791	100		
	1.0	1.29	101		

a. Average value for 3 determinations
b. Diluted 10 times
c. Not detected

5.4. Conclusion

A SI-based SPE system coupled with GFAAS (Auto-Pret-GFAAS system) for trace cadmium, and lead was developed and its operating parameters were optimized and all operations including preconcentration and detection were carried out automatically by home-made software. The sensitivity and selectivity of the proposed method are

comparable to those by ICP-MS. This method was applied to the determination of cadmium and lead in tap water and in the leached solutions from ceramic ware using 4% acetic acid. By the proposed method, it became possible to determine cadmium at ng L^{-1} and lead at μg L^{-1} level.

Chapter 6 Exploiting a simple water extract of a flower as a natural reagent for acidity assay using a lab-on-chip[142]

6.1. Introduction

In chemical analysis, many chemicals are used and wasted. In some cases toxic chemicals causing contamination of the environment are used. From the point of view of green chemistry, it is desirable that these wastes are reduced.

Manz *et al.*[38] proposed the concept of micro total analysis system (μTAS) in 1990. In μTAS called on lab-on-a-chip, all devices such as a pump, a valve and a detector are integrated on a small chip, and therefore, it has great advantage in the reduction of reagent consumption, simplicity of the analysis system and rapidity of the analysis. The field of μTAS has been growing rapidly and the trend of this field was reviewed.[39-41] Recently, Grudpan *et al.*[143] developed a simple and economical lab-on-chip (LOC) with time-based detection. Four chemical reactions were introduced into the LOC and it was applied to the determination of ascorbic acid, acetic acid and iron in real samples. But the colored reaction zone was detected visually by naked eyes and using a stopwatch.

The use of reagents from natural materials like plants is one of the environment-friendly methods. Uchiyama *et al.*[144,145] developed an amperometric flow injection (FI) analysis system using cucumber juice as a carrier solution for the measurement of ascorbic acid. Ascorbate oxidase in the cucumber catalyzes the oxidation of ascorbic acid. The oxygen consumed in this reaction was detected by an oxygen electrode. A guava leaf extract was exploited for FI determination of iron.[146] The guava leaf extract formed a colored complex with iron and it was detected by a spectrometer, and a normal FI system, a reverse FI system and a column FI system were

tested for the determination of iron at ppm levels. A green tea extract was also used for quantification of iron.[147]

Some plants contain water-soluble pigments like anthocyanin or betacyanin compounds.[148,149] The chemical structures of those pigments change depending on pH. Therefore, the extract containing anthocyanins or betacyanins can be used as pH indicator. Gomphrena globosa contains betacyanins in its petal.[150-153] The extract from it changes yellow in basic solution to reddish purple in acidic solution.

In the present study, a simple water extract of a flower was exploited as natural reagent for acidity assay. Acid-base neutralization reaction with the natural reagent was introduced into a simple LOC, and the color change was detected with a reflection/backscattering fiber optic probe coupled to a spectrometer. The natural reagent from Gomphrena globosa was obtained by simple extraction and its spectral characteristic was studied. The proposed method was applied to the determination of acetic acid in vinegar samples.

6.2. Experimental

6.2.1. *Reagents*

6.2.1.1. *Natural reagent*

A 0.7 g portion of dry petal of Gomphrena globosa was put into 50 mL of hot water at 60–70°C and kept for an hour. Boiling water is not suitable for extraction because the structure of the dye might change or decompose at the high temperature. After extraction, petals were removed by filtering the extract through filter paper. The extract

could be kept at least for three days in the refrigerator. Before loading it into the LOC system, it was adjusted to pH 9 using 1 M sodium hydroxide solution.

6.2.1.2. *Standard acetic acid solution*

A 20 % (w/w) stock solution of acetic acid was prepared by diluting glacial acetic acid (≧ 99%, Analytical reagent grade, LAB-SCAN, Ireland) with water. The standardization of the stock standard solution was carried out by the titration method using sodium hydroxide. Working solutions of acetic acid were daily prepared by dilution of the stock solution with water.

6.2.2. *Apparatus*

The diagram of the LOC system used in this work is shown in Fig. 6-1. This system consists of a chip unit (Fig. 6-2), two solenoid pumps, two solenoid valves and a detector. The LOC was made as described in a previous report.[143] The chip consists of an acrylic piece (2 cm × 3 cm × 1 cm) with two channels (1 mm i.d.) crossed perpendicularly. As shown in Fig. 6-2, the chip was tilted at 20° angle with respect to the horizontal in order to be in gravimetric force. The threads were made at each channel opening to fit a 1/4 inch nut. The chip was put between two acrylic pieces. The surface of the chip unit was colored black to avoid interference from outside light. A spectrophotometer (USB 2000, Ocean Optics Inc., USA) equipped with a reflection/backscattering fiber optic probe (R200-7-UV-VIS, Ocean Optics Inc., USA) and a tungsten halogen light source (LS-1-LL, Ocean Optics Inc., USA) was used for absorbance measurement. To place the fiber optic head at the detection point on the chip,

the top acrylic of the chip unit was drilled to provide a hole. The detection point was set about 5 mm down from the junction of the vertical channel and the horizonal channel. Two solenoid pumps (Biochem valve, USA) were used to load the natural reagent and the acetic acid standard/sample into each channel. Both pumps were connected to the inlets of the channels. Two solenoid valves (Takasago, Japan) were connected to outlets of the channels. These pumps and valves were controlled by switches.[154] FIAlab software was used to record absorbance spectra at the detection point.

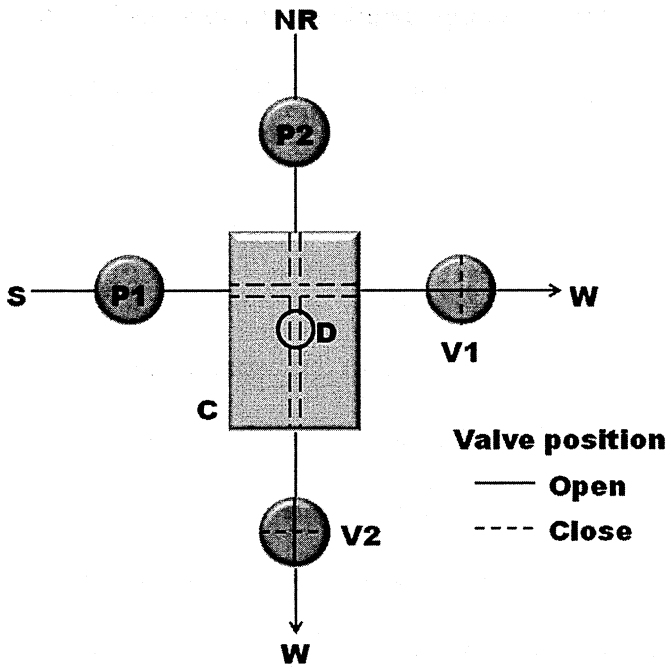

Fig. 6-1 Schematic diagram of the LOC system.

C: Chip, D: Detection point, P1 and P2: Solenoid pumps, V1 and V2: Solenoid valves, NR: Natural reagent, S: Sample/Standard, W: Waste

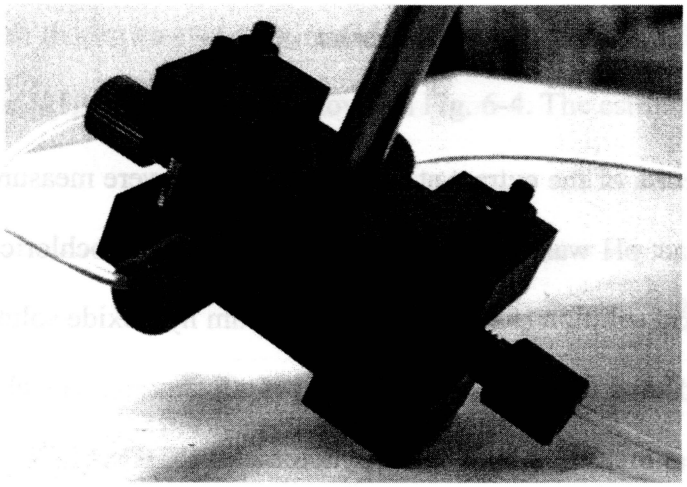

Fig .6-2 Photograph of the chip unit.

6.2.3. *Operating procedure*

First, V1 was opened and V2 was closed. An acetic acid standard/sample was loaded into the horizonal channel by P1. After that, V1 was closed and V2 was opened. The natural reagent adjusted to pH 9 was pumped into the vertical channel by P2. After loading the reagent, V2 was closed and V1 was opened again. P1 was switched once to load the standard/sample. At the same time, the program for measurement of absorbance spectra at the detection point was started. Afterward, V1 was closed immediately. The loaded acetic acid standard/sample migrated toward the detection point and merged with the natural reagent. The migration occurred from the difference in concentration of the reagent and sample zones which was helped by capillary action and gravimetric force[143] This resulted in the change in pH and the color of the natural reagent was changed.

6.3. Results and Discussion

6.3.1. *Spectral characteristics of the extract*

Absorption spectra of the extract at various pH values were measured by a batchwise method. The extract pH was adjusted from 1 to 13 using hydrochloric acid solution (for pH 1–3), acetic acid solution (for pH 4–6) and sodium hydroxide solution (for pH 7–13). The extract was diluted four folds through the pH adjustment. The absorption spectrum of the solution was measured by a spectrophotometer (SHIMADZU, UV-1800, Japan). As can be seen in Fig. 6-3, at lower pH, the extract has maximum absorption at 545 nm, and a red shift occurred with an increase in pH. On the other hand, the maximum absorption was observed at 360 nm in the basic solution. At pH 13, a blue shift was observed.

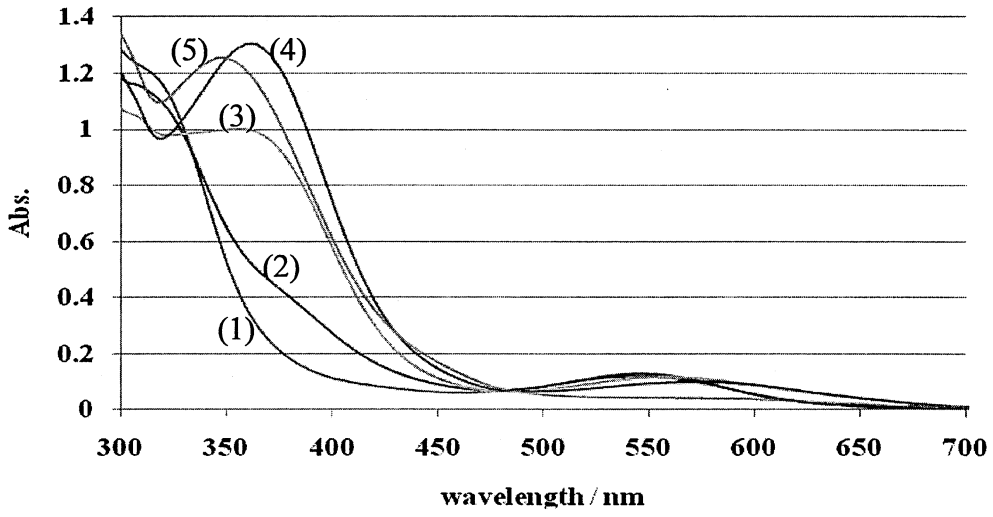

Fig. 6-3 Absorbance spectra of the extract from Gomphrena globosa at various pH value.

(1):pH1, (2):pH8, (3):pH9, (4):pH12, (5):pH13

The pK_a value of this extract was estimated from the intercept of the plot of pH as a function of log([In^-]/[HIn]). Results are shown in Fig. 6-4. The estimated pK_a was 9.48.

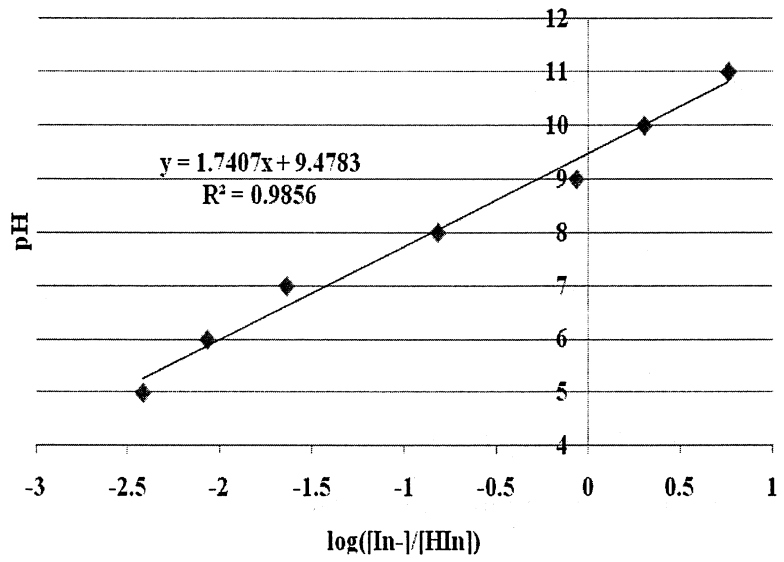

Fig. 6-4 A plot of pH as a function of log([In^-]/[HIn]).

6.3.2. *Starting pH of the natural reagent*

The starting pH of the natural reagent was chosen based on the characteristic spectra. A pH at or above 9 is suitable for acidity assay, as a change of the absorbance is observed at lower pH than pH 9. But the absorbance of the extract was unstable at pH above 11. Taking into consideration the spectral characteristics and the stability of the absorbance of the extract, we chose pH 9 as the starting pH.

6.3.3. *Selection of the waiting time before measurement and optimum wavelength*

Capillary action and gravimetric force caused the penetration of a loaded acetic acid standard solution into a natural reagent. Therefore, it was necessary to figure out the suitable waiting time which a sample zone passed through the detection point. We examined the effect of waiting time before the measurement of the absorption spectrum. The absorption spectra were measured at exactly 10, 15, 20 and 25 s after the loading of acetic acid standard solutions in the range of 1–7% (w/w). Based on the results, we prepared calibration curves for acetic acid with different wavelengths (400–600 nm). Linearity and repeatability of the calibration curves at various conditions are shown in Table 6-1. The better calibration curve was obtained at 15 s for the waiting time and 580 nm for the wavelength. The data source of the calibration curve is shown in Fig. 6-5. As can be seen in Fig. 6-5, the absorbance at 580 nm decreased proportionally to the concentration of acetic acid.

Table 6-1 Correlation coefficient values of calibration curves for acetic acid and repeatability at various conditions

Waiting	400 nm		545 nm		580 nm		600 nm	
time / s	r^2 [a]	RSD[b], %	r^2 [a]	RSD[b], %	r^2 [a]	RSD[b], %	r^2 [a]	RSD[b], %
10	0.668	18.1	0.902	3.27	0.922	4.18	0.800	10.6
15	0.910	21.0	0.932	3.11	0.999	2.55	0.957	9.63
20	0.742	14.7	0.948	4.25	0.862	5.11	0.706	10.5
25	0.584	10.7	0.957	4.11	0.896	4.10	0.780	8.83

a. Correlation coefficient values of calibration curves for 1–7% (w/w) acetic acid.

b. Relative standard deviation values of ten determinations of 5% (w/w) acetic acid.

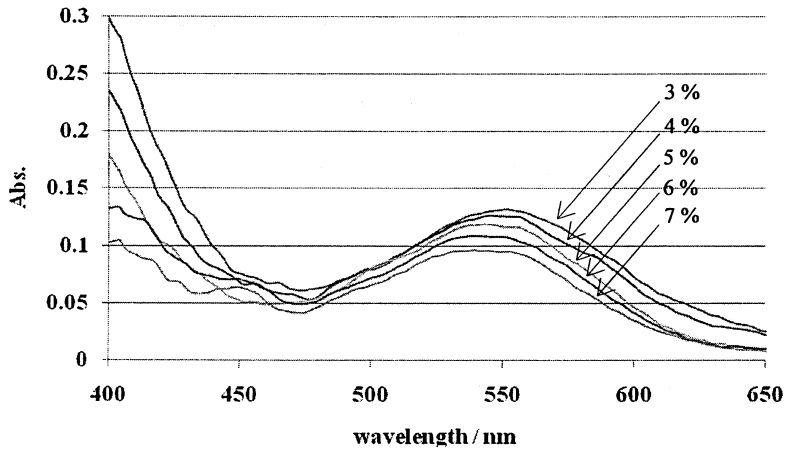

Fig. 6-5 Absorbance spectra at the detection point (the spectra were measured exactly 15 s after the loading acetic acid solution).

6.3.4. *Calibration curve for acetic acid*

A liner calibration curve for acetic acid was obtained in the range of 3 to 7 % (w/w). The equation was $Y = -0.0110X + 0.137$ with a correlation coefficient of 0.999, where Y is the absorbance at 580 nm and X is the concentration of acetic acid in % (w/w). The relative standard deviation was 2.55 % for ten determinations of 5 % acetic acid standard solution.

6.3.5. *Application*

This LOC system using natural reagent was applied to the determination of acetic acid in vinegar samples. All samples were purchased from a store and labeled as 5% (w/w). The analytical values were obtained by the calibration curve method. Results are summarized in Table 6-2. A paired *t*-test was performed on the data obtained by the

proposed method and the titration method. The experimental *t*-value was 1.350 which is less than the critical *t*-value at the 95% confidence level for four degrees of freedom (2.776). The statistical analysis revealed that there is no significant difference between the two methods.

Table 6-2 Determination of acetic acid in vinegar samples.

Sample	Concentration of acetic acid / % (w/w)[a]	
	Proposed method	Titration method
1	4.55±0.17	4.37±0.04
2	5.19±0.21	5.04±0.01
3	5.24±0.21	5.41±0.03
4	5.20±0.13	5.13±0.03
5	5.66±0.14	5.37±0.01

a. Average value and standard deviation for three determinations.

6.4. Conclusion

The acidity assay using the simple LOC with the natural reagent was demonstrated. The proposed method was applied to the acetic acid determination in vinegar samples. This method is a cost-effective and environment-friendly analysis. The use of the natural reagent is expected to be applied to the other chemical analysis.

Chapter 7 Conclusions

Nowadays, a simple, rapid and sensitive method for trace analysis is required. And it is desirable that reagent and sample consumption and waste generation are reduced. In this study, semi- and fully automated analysis systems based on the flow-based techniques were developed.

In the chapter 2, a spectrophotometric flow injection analysis (FIA) was investigated for formaldehyde (HCHO) in industrial wastewater. HCHO was condensed with hydroxylamine, and then the residual hydroxylamine reduced iron(III)-ferrozine complex. As a result, iron(II)-ferrozine complex was formed and detected at 562 nm. The chemical reaction was introduced into FIA system with high precision. This method is capable of monitoring wastewater.

In the chapter 3, a new HCHO standard gas generator based on gravitational dispensing-vaporization and an automated FIA equipped with diffusion scrubber for the gaseous HCHO were developed. The proposed system could determine trace breath HCHO with 3 min intervals. And also, the concentration of standard gas generated by the proposed method was verified by 2,4-dinitrophenylhydrazine-HPLC method and this standard gas generator was effective for the calibration in the FIA system.

In the chapter 4, an automatic stopped-in-dual-loop flow analysis (SIDL-FA) system was proposed. The detectable reaction for vanadium is based on its catalytic effect on the oxidation of *p*-anisidine by bromate in the presence of Tiron as an activator. The catalytic reaction was accelerated in the loop on the six-way valve and all pumps were stopped while the catalytic reaction occurred. This procedure leads to reduce reagent consumption and waste generation. The proposed method was applied to the determination of trace vanadium in drinking water.

In the chapter 5, a fully automated pre-concentration system coupled with graphite furnace atomic absorption spectrometry (GFAAS) was developed for enhancement of sensitivity. A handmade minicolumn packed with a chelating resin (NOBIAS CHELATE-PA1) was used for the pre-concentration of cadmium and lead. All protocol for the on-line SPE method was controlled by home-made software. A trigger switch that was placed aside the graphite furnace was used to synchronize the home-made software with built-in one in the GFAAS. The proposed Auto-Pret-GFAAS system showed high sensitivity comparable to ICP-MS. Cadmium and lead at the level of ppt in the leached solutions was detectable utilizing the Auto-Pret-GFAAS system.

In the chapter 6, a simple and economic lab-on-chip was contrived for an acidity assay. This system was small compared with other FIA and SIA system and extremely it could reduce reagent consumption and waste generation. In addition, an extract of a flower was used as a natural reagent. Therefore, this method was environment-friendly.

Proposed flow-based techniques have big advantages in the simplicity, rapidity and sensitivity over conventional ones, and also are expected to be applied to various samples such as environmental and biological samples.

On the life innovation in the future, it is necessary and important to preserve our environment and protect our life in the world. Accordingly, high technology on trace analysis and speciation is needed. Environment-friendly and micro flow-based technique can develop besides.

References

1. J. Ruzicka, E. H. Hansen, *Anal. Chim. Acta*, **1975**, *78*, 145.
2. J. Ruzicka, G. D. Marshall, *Anal. Chim. Acta*, **1990**, *273*, 329.
3. P. K. Dasgupta, *Atmos. Environ.*, **1984**, *18*, 1593.
4. Q. Fan, P. K. Dasgupta, *Anal. Chem.*, **1994**, *66*, 551.
5. J. Li, P. K. Dasgupta, Z. Genfa, M. A. Hutterli, *Field Anal. Chem. Technol.*, **2001**, *5*, 2.
6. K. Toda, K. Yoshioka, K. Mori. S. Hirata, *Anal. Chim. Acta*, **2005**, *531*, 41.
7. K. Toda, S. Ohira, T. Tanaka, T. Nishimura, P. K. Dasgupta, *Environ. Sci. Technol.*, **2004**, *38*, 1529.
8. N. Teshima, S. Ohno, T. Sakai, *Anal.Sci.*, **2007**, *23*, 1.
9. T. Sakai, S. Fujimoto, K. Higuchi, N. Teshima, *Bunseki Kagaku*, **2005**, *54*, 1183.
10. M. Kuramochi, K. Tomioka, M. Fujinami, K. Oguma, *Talanta*, **2005**, *68*, 287.
11. K. Fukui, S. Ohno, K. Higuchi, N. Teshima, T. Sakai, *Bunseki Kagaku*, **2007**, *56*, 757.
12. K. Jitmanee, M. Oshima, S. Motomizu, *J. Flow Injection Anal.*, **2004**, *21(1)*, 49.
13. H. Karami, M. F. Mousavi, Y. Yamini, M. Shamsipur, *Anal. Chim. Acta*, **2004**, *509*, 89.
14. K. Jitmanee, M. Ohshima, S. Motomizu, *Talanta*, **2005**, *66*, 529.
15. T. Yamamoto, A. Sabarudin, O. Noguchi, T. Takayanagi, M. Oshima, S. Motomizu, *Bunseki Kagaku*, **2006**, *55*, 715.
16. A. Sabarudin, N. Lenghor, Y. Liping, Y. Furusho, S. Motomizu, *Spectrosc. Lett.*, **2006**, *39*, 669.
17. R. K. Katarina, N. Lenghor, S. Motomizu, *Anal.Sci.*, **2007**, *23*, 343.

18. R. K. Katarina, L Hakim, M. Oshima, S. Motomizu, *J. Flow Injection Anal.*, **2008**, *25(2)*, 166.

19. K. Oshita, M. Oshima, Y. Gao, K. Lee, S. Motomizu, *J. Flow Injection Anal.*, **2002**, *19(2)*, 143.

20. S. Motomizu, K. Jitmanee, M. Oshima, *Anal. Chim. Acta*, **2003**, *499*, 149.

21. J. Yin, Z. Jiang, G. Chang, B. Hu, *Anal. Chim. Acta*, **2005**, *540*, 333.

22. L.-S. Huang, K.-C. Lin, *Anal.Sci.*, **2006**, *22*, 1375.

23. K. Jitmanee, N. Teshima, T. Sakai, K. Grudpan, *Talanta*, **2007**, *73*, 352.

24. Y. Bakircioglu, S. R. Segade, E. R. Yourd, J. F. Tyson, *Anal. Chim. Acta*, **2003**, *485*, 9.

25. R. Chomchoei, M. Miró, E. H. Hansen, J. Shiowatana, *Anal. Chem.*, **2005**, *77*, 2720.

26. S. Walas, A. Tobiasz, M. Gawin, B. Trzewik, M. Strojny, H. Mrowiec, *Talanta*, **2008**, *76*, 96.

27. R. M. Cespón-Romero, M. C. Yebra-Biurrun, *Anal. Chim. Acta*, **2008**, *609*, 184.

28. I. S. I. Adam, A. N. Anthemidis, *Talanta*, **2009**, *77*, 1160.

29. E. M. Martinis, R. A. Olsina, J. C. Altamirano, R. G. Wuilloud, *Talanta*, **2009**, *78*, 857.

30. D. Kara, *Talanta*, **2009**, *79*, 429.

31. Y. Hirano, H. Sakurai, A. Endo, K. Oguma, Y. Terui, *Bunseki Kagaku*, **2001**, *50*, 885.

32. Y. Hirano, J. Nakajima, K. Oguma, Y. Terui, *Anal.Sci.*, **2001**, *17*, 1073.

33. Y.-H. Sung, S.-D. Huang, *Anal. Chim. Acta*, **2003**, *495*, 165.

34. P. Ampan, J. Ruzicka, R. Atallah, G. D. Christian, J. Jakmunee, K. Grudpan, *Anal. Chim. Acta*, **2003**, *499*, 167.

35. J. Nakajima, Y. Hirano, K. Oguma, *Anal.Sci.*, **2003**, *19*, 585.

36. X. Long, M. Miró, E. H. Hansen, *Anal. Chem.*, **2005**, *77*, 6032.

37. A. N. Anthemidis, I. S. I. Adam, *Anal. Chim. Acta*, **2009**, *632*, 216.

38. A. Manz, N. Graber, H. M. Widmer, *Sens. Actuators B*, **1990**, *1*, 244.

39. D. R. Reyes, D Iossifidis, P. Auroux, A. Manz, *Anal. Chem.*, **2002**, *74*, 2623.

40. P. Auroux, D. Iossifidis, D. R. Reyes, A. Manz, *Anal. Chem.*, **2002**, *74*, 2637.

41. T. Vilkner, D. Janasek, A. Manz, *Anal. Chem.*, **2002**, *76*, 3373.

42. N. Teshima, S. K. M. Fernández, M. Ueda, H. Nakai, T. Sakai, *Talanta*, accepted.

43. WHO Regional Publications, European Series, No. 91, Air Quality Guidelines for Europe, F. Theakston (Ed.), 2nd ed., **2000**, World Health Organization Regional Office for Europe, Copenhagen, 87.

44. Environmental Quality Standards of Japan, Environmental Quality Standards for Water Pollution, http://www.env.go.jp/en/water/wq/wp.pdf, last accessed June 18, **2010**.

45. K. Murai, M. Okano, H. Kuramitz, N. Hara, T. Kawakami, S. Taguchi, *Anal. Sci.*, **2008**, *24*, 1455.

46. T. Nash, *Biochem. J.*, **1953**, *55*, 416.

47. T. Sakai, S. Tanaka, N. Teshima, S. Yasuda, N. Ura, *Talanta*, **2002**, *58*, 1271.

48. M. Ueda, N. Teshima, T. Sakai, *Bunseki Kagaku*, **2008**, *57*, 605.

49. H. Nishikawa, H. Nagasawa, T. Sakai, *Bunseki Kagaku*, **1998**, *47*, 225.

50. Q. Li, P. Sritharathikhun, S. Motomizu, *Anal. Sci.*, **2007**, *23*, 413.

51. Q. Li, P. Sritharathikhum, M. Oshima, S. Motomizu, *Anal. Chem. Acta*, **2008**, *612*, 165.

52. S. Teerasong, N. Amornthammarong, K. Grudpan, N. Teshima, T. Sakai, D. Nacapricha, N. Ratanawimarnwong, *Anal. Sci.*, **2010**, *26*, 629.

53. N. Nakano, M. Ishikawa, Y. Kobayashi, K. Nagashima, *Anal. Sci.*, **1994**, *10*, 641.

54. H. Nakai, N. Teshima, T. Sakai, *Bunseki Kagaku*, **2010**, *59*, 273.

55. G. G. Rao, G. Somidevamma, *Fresenius' J. Anal. Chem.*, **1959**, *165*, 432.

56. L. L. Stookey, *Anal. Chem.*, **1970**, *42*, 779.

57. Commentary of JIS K 0102, "*Testing methods for industrial wastewater*", 2008, Japanese Industrial Standards Committee, Tokyo.

58. H. Hori, K. Arashidani, *J. UOEH*, **1997**, *19*, 123.

59. S. Ohira, K. Someya, K. Toda, *Anal. Chim. Acta*, **2007**, *588*, 147.

60. D. Smith, P. Spanel, *Analyst*, **2007**, *132*, 390.

61. W. Miekisch, J. K. Schubert, G. F. E. Noeldge-Schomburg, *Clin. Chim. Acta*, **2004**, *347*, 25.

62. J. D. Fenske, S. E. Paulson, *J. Air Waste Manage. Assoc.*, **1999**, *49*, 594.

63. M. J. Henderson, B. A. Karger, G. A. Wrenshall, *Diabetes*, **1952**, *1*, 188.

64. T. Ligor, J. Szeliga, M. Jackowski, B. Buszewski, *J. Breath Res.*, **2007**, *1*, 016001.

65. M. Phillips, R. N. Cataneo, R. Condos, G. A. R. Erickson, J. Greenberg, V. L. Bombardi, M. I. Munawar, O. Tietje, *Tuberculosis*, **2007**, *87*, 44.

66. M. Phillips, J. Herrera, S. Krishnan, M. Zain, J. Greenberg, R. N. Cataneo, *J. Chromatogr. B*, **1999**, *729*, 75.

67. O. Laakso, M. Haapala, T. Kuitunen, J. Himberg, *J. Anal. Toxicol.*, **2004**, *28*, 111.

68. O. Laakso, M. Haapala, P. Jaakkola, R. Laaksonen, K. Luomanmaki, J. Nieminen, M. Pettersson, H. Paiva, M. Rasanen, J. Himberg, *J. Anal. Toxicol.*, **2001**, *25*, 26.

69. P. Lirk, F. Bodrogi, M. Deibl, C. M. Kaehler, M. Joshua, B. Moser, G. Pinggera, H. Raifer, J. Rieder, W. Schobersberger, *Wiener Klinische Wochenschrift*, **2004**, *116*, 21.

70. J. Rieder, P. Lirk, C. Ebenbichler, G. Gruber, P. Prazeller, W. Lindinger, A. Amann,

Wiener Klinische Wochenschrift, **2001**, *113*, 181.

71. R. N. Bloor, P. Spanel, D. Smith, *Addiction Biology*, **2006**, *11*, 163.
72. S. M. Abbott, J. B. Elder, P. Spanel, D. Smith, *Int. J. Mass Spectrom.*, **2003**, *228*, 655.
73. S. T. Senthilmohan, M. J. McEwan, P. F. Wilson, D. B. Milligan, C. G. Freeman, *Redox Report*, **2001**, *6*, 185.
74. N. Teshima, J. Li, K. Toda, P. K. Dasgupta, *Anal. Chim. Acta*, **2005**, *535*, 189.
75. K. Toda, J. Li, P. K. Dasgupta, *Anal. Chem.*, **2006**, *78*, 7284.
76. S. Ohira, J. Li, W. A. Lonneman, P. K. Dasgupta, K. Toda, *Anal. Chem.*, **2007**, *79*, 2641.
77. E. G. Vasiliou, Y. M. Makarovska, I. A. Pneumatikos, N. V. Lolis, E. A. Kalogeratos, E. K. Papadakis, C. A. Georgiou, *J. Braz. Chem. Soc.*, **2007**, *18*, 1040.
78. P. Spanel, D. Smith, T. A. Holland, W. A. Singary, J. B. Elder, *Rapid Commun. Mass Spectrom.*, **1999**, *13*, 1354.
79. A. Wehinger, A. Schmid, S. Mechtcheriakov, M. Ledochowski, C. Grabmer, G. A. Gastl, A. Amann, *Int. J. Mass Spectrom.*, **2007**, *265*, 49.
80. C. Turner, B. Parekh, C. Walton, P. Spanel, D. Smith, M. Evans, *Rapid Commun. Mass Spectrom.*, **2008**, *22*, 526.
81. A. M. Diskin, P. Spanel, D. Smith, *Physio. Meas.*, **2003**, *24*, 107.
82. N. Teshima, M. Kuno, M. Ueda, H. Ueda, S. Ohno, T. Sakai, *Talanta*, **2009**, *79*, 517.
83. M. D. V. Badmaev, P. Subbalakshmi, M. Muhammed, *J. Altern. Complement. Med.*, **1999**, *5*, 273.
84. H. Ueki, *Yakugaku Zasshi*, **2003**, *123*, 633.

85. C. E. Heyliger, A. G. Tahiliani, J. H. McNeill, *Nature*, **1985**, *227*, 1474.

86. K. Cusi, S. Cukier, R. A. Defronzo, M. Torres, F. M. Puchulu, J. C. P. Redondo, *J. Clin. Endocrinol. Metab.*, **2001**, *86*, 1410.

87. A. B. Goldfine, D. C. Simonson, F. Folli, M.-E. Patti, C. R. Kahn, *Mol. Cell. Biochem.*, **1995**, *153*, 217.

88. O. Jacques-Camarena, M. González-Ortiz, E. Martínez-Abundis, J. F. P. López-Madrueño, R. Medina-Santillán, *Ann Nutr Metab*, **2008**, *53*, 195.

89. S. Wild, G. Roglic, A. Green, R. Sicree, H. King, *Diabetes Care*, **2004**, *27*, 1047.

90. T. Kitta, S. Yamada, T. Asakawa, K. Ishihara, N. Watanabe, H. Ishiyama, Y. Watanabe, *Oyo Yakuri/Pharmacometrics*, **2003**, *64*, 77.

91. S. R. Crouch, A. Scheeline, E. S. Kirkor, *Anal. Chem.*, **2000**, *72*, 53R.

92. T. Kawashima, N. Teshima, S. Nakano, Catalytic Kinetic Determinations: Nonenzymatic, in: R.A. Meyers (Ed.), Encyclopedia of Analytical Chemistry, John Wiley & Sons, Chichester, **2000**, p. 11034.

93. P. R. Bontschev, *Microchim. Acta*, **1962**, *50*, 577.

94. G. D. Christian, *Anal. Lett.*, **1971**, *4*, 187.

95. M. L. Camacho, M. T. Rodriguez, M. C. Mochón, A. G. Perez, *Anal. Chim. Acta*, **1991**, *244*, 89.

96. J. Gao, X. Zhang, W. Yang, B. Zhao, J. Hou, J. Kang, *Talanta*, **2000**, *51*, 447.

97. A. A. Mohamed, K. F. Fawy, *J. Trace Microprobe Tech.*, **2002**, *20*, 29.

98. T. Sakai, N. Teshima, *Anal. Sci.*, **2008**, *24*, 855.

99. T. Yamane, T. Fukasawa, *Anal. Chim. Acta*, **1980**, *119*, 389.

100. T. Fukasawa, S. Kawakubo, T. Okabe, A. Mizuike, *Bunseki Kagaku*, **1984**, *33*, 609.

101. S. Nakano, M. Tago, T. Kawashima, *Anal. Sci.*, **1989**, *5*, 69.

102. A. A. Ensafi, A. Kazemzadeh, *Microchem. J.*, **1996**, *53*, 139.

103. S. Kawakubo, K. Kajihara, M. Iwatsuki, *Anal. Sci.*, **1996**, *12*, 237.

104. T. Shiobara, N. Teshima, M. Kurihara, S. Nakano, T. Kawashima, *Talanta*, **1999**, *49*, 1083.

105. S. Nakano, E. Tanaka, Y. Mizutani, *Talanta*, **2003**, *61*, 203.

106. S. Nakano, N. Teshima, M. Kurihara, T. Kawashima, *Bunseki Kagaku*, **2004**, *53*, 255.

107. S. Nakano, K. Sakamoto, A. Takenobu, T. Kawashima, *Talanta*, **2002**, *58*, 1263.

108. J. A. P. Pérez, J. S. D. Alegría, P. F. Hernando, A. N. Sierra, *Anal. Chim. Acta*, **2005**, *536*, 115.

109. K. Petersen, P. K. Dasgupta, *Talanta*, **1989**, *36*, 49.

110. B. F. Reis, M. F. Giné, E. A. G. Zagatto, J. L. F. C. Lima, R. A. Lapa, *Anal. Chim. Acta*, **1994**, *293*, 129.

111. V. Cerda, J. M. Estela, R. Forteza, A. Cladera, E. Becerra, P. Altimira, P. Sitjar, *Talanta*, **1999**, *50*, 695.

112. H. Itabashi, H. Kawamoto, T. Kawashima, *Anal. Sci.*, **2001**, *17*, 229.

113. R. A. S. Lapa, J. L. F. C. Lima, B. F. Reis, J. L. M. Santos, E. A. G. Zagatto, *Anal. Chim. Acta*, **2002**, *466*, 125.

114. N. Amornthammarong, J. Jakmunee, J. Li, P. K. Dasgupta, *Anal. Chem.*, **2006**, *78*, 1890.

115. P. R. Fortes, S. R. P. Meneses, E. A. G. Zagatto, *Anal. Chim. Acta*, **2006**, *572*, 316.

116. K. Grudpan, *Talanta*, **2004**, *64*, 1084.

117. P. R. Bontschev, B. G. Jeliazkowa, *Microchim. Acta*, **1967**, *55*, 116.

118. P. R. Bontschev, *Talanta*, **1972**, *19*, 675.

119. P. R. Bontchev, B. G. Jeliazkowa, *Inorg. Chim. Acta*, **1967**, *1*, 249.

120. P. R. Bontchev, G. S. Nikolov, *J. Inorg. Nucl. Chem.*, **1966**, *28*, 2609.

121. K. Watla-iad, T. Sakai, N. Teshima, S. Katoh, K. Grudpan, *Anal. Chim. Acta*, **2007**, *604*, 139.

122. S. Ohno, M. Tanaka, N. Teshima, T. Sakai, *Anal. Sci.*, **2004**, *20*, 171.

123. M. Ueda, N. Teshima, T. Sakai, Y. Joichi, S. Motomizu, *Anal. Sci.*, **2010**, *26*, 597.

124. S. Olsen, L. R. Pessenda, J. Ruzicka, E. H. Hansen, *Analyst*, **1983**, *108*, 905.

125. M. Trojanowics, "*Flow injection analysis – Instrumentation and applications*", World Scientific, **2000**.

126. S. D. Kolev, I. D. McKelvie, "*Advances in flow injection analysis and related techniques*", Elsevier, **2008**.

127. T. Yamane, M. Izawa, S. Osada, *Bull. Soc. Sea Water Sci. Jpn*, **2006**, *60*, 352.

128. T. Yamane, Y. Kouzuka, M. Hirokawa, *Talanta*, **2001**, *55*, 387.

129. Y. Narusawa, *Anal. Chim. Acta*, **1988**, *204*, 53.

130. K. Grudpan, N. Warakijcharoenchai, O. Tue-Ngeun, P. Sooksamiti, J. Jakmunee, *ScienceAsia*, **1999**, *25*, 99.

131. T. Yamane, Y. Yamaguchi, *Anal. Chim. Acta*, **1997**, *345*, 139.

132. T. Seki, H. Takigawa, Y. Hirano, Y. Ishibashi, K. Oguma, *Anal. Sci.*, **2000**, *16*, 513.

133. G. A. Zachariadis, A. N. Anthemidis, P. G. Bettas, J. A. Stratis, *Talanta*, **2002**, *57*, 919.

134. S. Dadfarnia, I. Green, C. W. McLeod, *Anal. Proc.Incl. Anal. Commun.*, **1994**, *31*, 61.

135. Z. Sperling, X. Yin, B. Welz, *J. Anal. At. Spectrom.*, **1991**, *6*, 295.

136. J. Wang, E. H. Hansen, *TrAC, Trends in Anal. Chem.*, **2003**, *22*, 836.

137. A. Economou, *TrAC, Trends in Anal. Chem.*, **2005**, *24*, 416.

138. S. C. Hight, *J. AOAC Int.*, **2000**, *83*, 1174.

139. S. C. Hight, *J. AOAC Int.*, **2001**, *84*, 861.

140. H. Sakamoto, K. Yamamoto, T. Shirasaki, Y. Inoue, *Bunseki Kagaku*, **2006**, *55*, 133.

141. Commentary of JIS S 2400, "*Heat resistant ceramic tablewares*", **2000**, Japanese Industrial Standards Committee, Tokyo.

142. M. Ueda, S. Lapanantnoppakhun, W. Wongwilai, N. Teshima, T. Sakai, K. Grudpan, *J. Flow Injection Anal.*,**2010**, *27(1)*, 57.

143. K. Grudpan, S. Lapanantnoppakhun, S. K. Hartwall, K. Watla-iad, W. Wongwilai, W. Siriangkhawut, W. Jangbai, W. Kumutanat, P. Nuntaboon, S. Tontrong, *Talanta*, **2009**, *79*, 990.

144. S. Uchiyama, Y. Tofuku, S. Suzuki, *Anal. Chim. Acta*, **1988**, *208*, 291.

145. S. Uchiyama, S. Suzuki, *Bunseki Kagaku*, **1990**, *39*, 793.

146. T. Settheeworrarit, S. K. Hartwell, S. Lapanantnoppakhun, J. Jakmunee, G. D. Christian, K. Grudpan, *Talanta*, **2005**, *68*, 262.

147. P. Pinyou, S. K. Hartwell, J. Jakmunee, S. Lapanantnoppakhun, K. Grudpan, *Anal. Sci.*, **2010**, *26*, 619.

148. J. Kong, L. Chia, N. Goh, T. Chia, R. Brouillard, *Phytochemistry*, **2003**, *64*, 923.

149. D. Stract, T. Vogt, W. Schliemann, *Phytochemistry*, **2003**, *62*, 247.

150. M. Piattelli, L. Minale, *Phytochemistry*, **1964**, *3*, 547.

151. L. Minale, M. Piattelli, S. De Stefano, *Phytochemistry*, **1967**, *6*,703.

152. S. Heuer, V. Wray, J. W. Metzger, D. Strack, *Phytochemistry*, **1992**, *31*, 1801.

153. Y. Cai, M. Sun, H. Corke, *J. Agric. Food Chem.*, **2001**, *49*, 1971.

154. W. Wongwilai, S. Lapanantnoppakhun, S. Grudpan, K. Grudpan, *Talanta*, **2010**, *81*, 1137.

Acknowledgement

I deeply wish to express my sincere thanks to Prof. Tadao Sakai and Assoc. Prof. Norio Teshima of Department of Applied Chemistry, Aichi Institute of Technology for many useful advices and discussions.

I appreciate Emeritus Prof. of Nagoya University, Shin Tsuge and Prof. Shin-ichi Inoue of Aichi Institute of Technology for reviewing Ph.D thesis.

I am express my sincere thanks to Prof. Kei Toda of Graduate School of Science and Technology, Kumamoto University for a preparation of a diffusion scrubber used in this study and Mr. Ken-ichi Sugimoto of Aichi Industrial Technology Institute for valuable advices to the measurement of DNPH-HPLC method.

I am grateful to Prof. Shoji Motomizu and Mr. Yasutaka Joichi of Graduate School of Natural Science and Technology, Okayama University for technical supports and advices to a development of Auto-Pret sysem.

I express my deepest appreciation to Prof. Kate Grudpan, Assoc. Prof. Somchai Lapanantnoppakhun and Mr. Wasin Wongwilai of Department of Chemistry, Faculty of Science, Chiang Mai University in Thailand for various suggestions and supports to my research done in Chiang Mai University.

Sincere thanks are due to Dr. Shinsuke Ohno of Mitsubishi Chemical Analytech Co., Ltd., Ms. Masami Kuno, Mr. Hisashi Ueda, Ms. Sara Keiko Murase Fernández and Mr. Hirokazu Nakai for many supports on this study.

List of publications

1. 上田　実, 手嶋紀雄, 酒井忠雄

   重力滴下-蒸発法によるホルムアルデヒド標準ガス発生法の開発と呼気ホルムアルデヒド分析への応用, *分析化学*, **2008**, *57*, 605–611

2. Norio Teshima, Masami Kuno, Minoru Ueda, Hisashi Ueda, Shinsuke Ohno, Tadao Sakai

   Automated stopped-in-dual-loop flow analysis system for catalytic determination of vanadium in drinking water, *Talanta*, **2009**, *79*, 517–522

3. Minoru Ueda, Norio Teshima, Tadao Sakai, Yasutaka Joichi, Shoji Momomizu

   Highly sensitive determination of cadmium and lead in leached solutions from ceramic ware by graphite furnace atomic absorption spectrometry coupled with sequential injection-based solid phase extraction method, *Anal. Sci.*, **2010**, *26*, 597–602

4. Minoru Ueda, Somchai Lapanantnoppakhun, Wasin Wongwilai, Norio Teshima, Tadao Sakai, Kate Grudpan

   Exploiting a simple water extract of a flower as a natural reagent for acidity assay using a lab-on-chip, *J. Flow Injection Anal.*, **2010**, *27*, 57–60

5. Norio Teshima, Sara Keiko Murase Fernández , Minoru Ueda, Hirokazu Nakai,Tadao Sakai

   Flow injection spectrophotometric determination of formaldehyde based on its condensation with hydroxylamine and subsequent redox reaction with iron(III)-ferrozine complex, *Talanta,* accepted.